SK でのステライルおよび非標準的相互作用に関する制限

Limits on Sterile Neutrinos and Non-Standard Neutrino Interactions at SK

Euan Richard (ICRR, University of Tokyo)
2015/02/21

Contents

- Quick introduction to SK data
- SK searches:
  - **Sterile neutrino oscillation** (A. Himmel, Duke U.)
    http://arxiv.org/abs/1410.2008
  - **MeV sterile decay** (E. Richard, RCCN)
  - **Non Standard Neutrino Interactions** (G. Mitsuka, RCCN)
    http://arxiv.org/abs/1109.1889
  - **Lorentz Invariance Violation** (T. Akiri and A. Himmel, Duke U.)
    http://arxiv.org/abs/1410.4267

Thanks especially to A. Himmel for providing many of the slides and figures.

Introduction to SK

Super-Kamiokande

- Atmospheric dataset provides access to wide range of *L* and *E*.

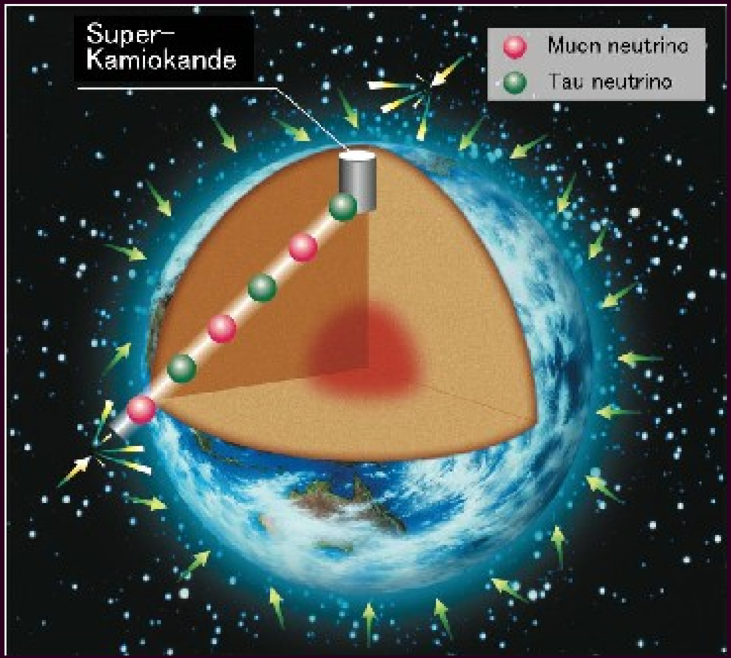

$P(\nu_\mu \rightarrow \nu_\mu)$

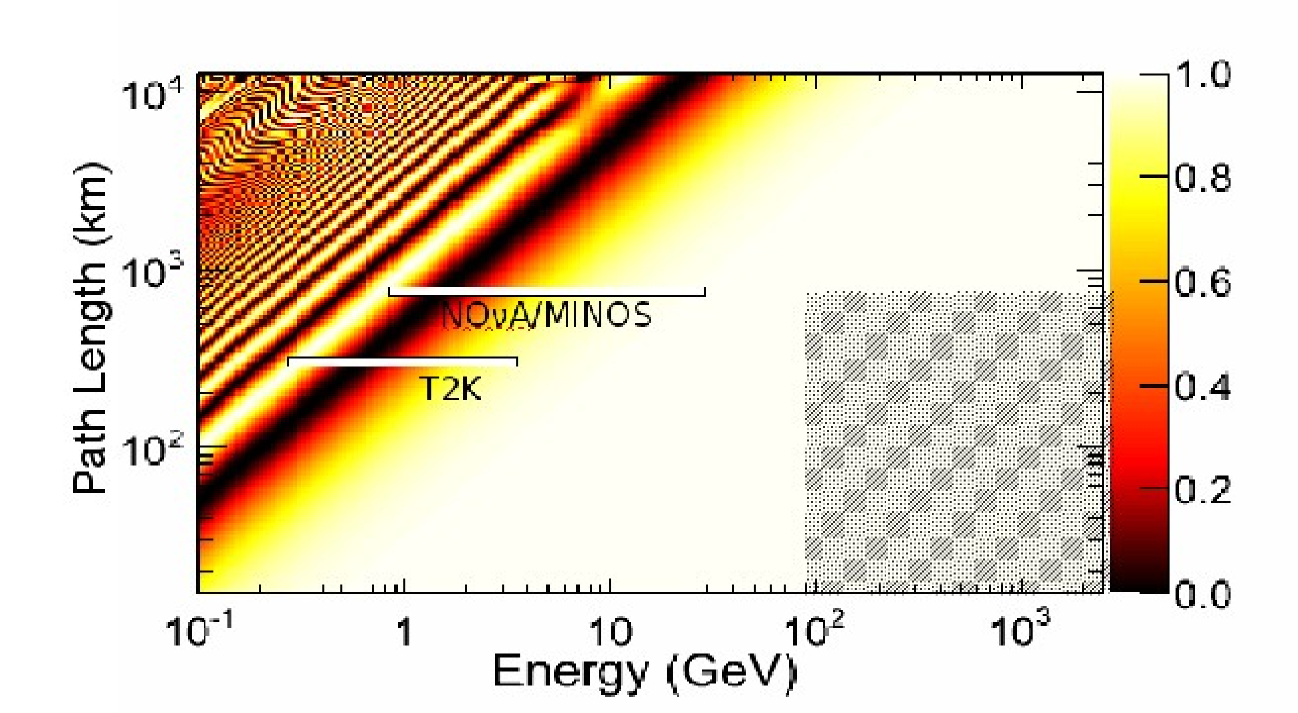

Particle Identification

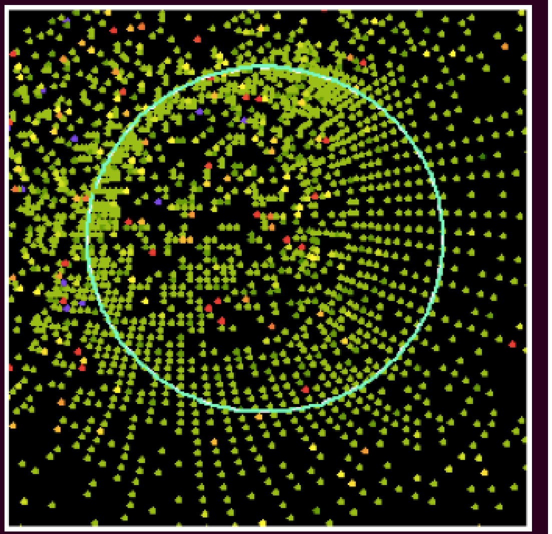

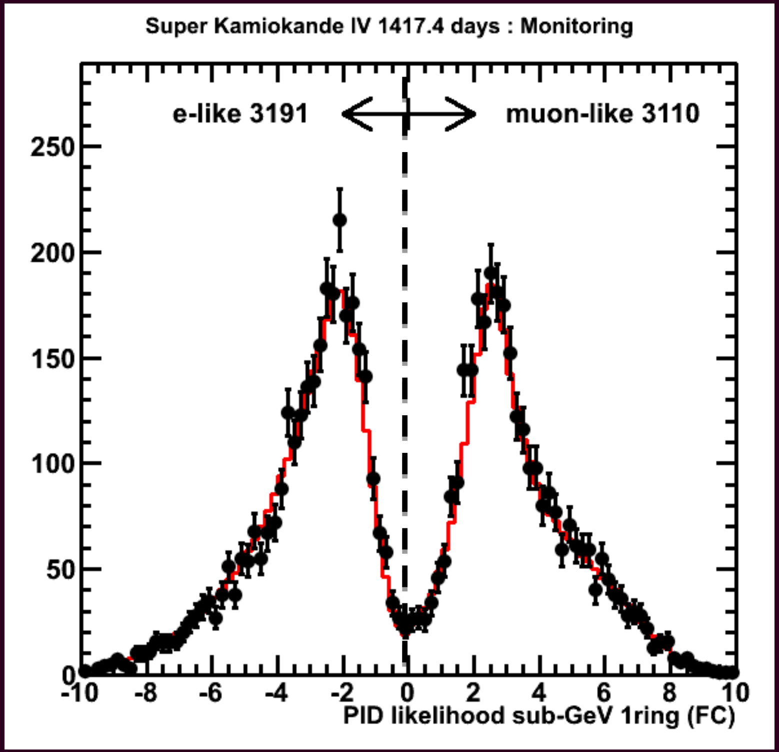

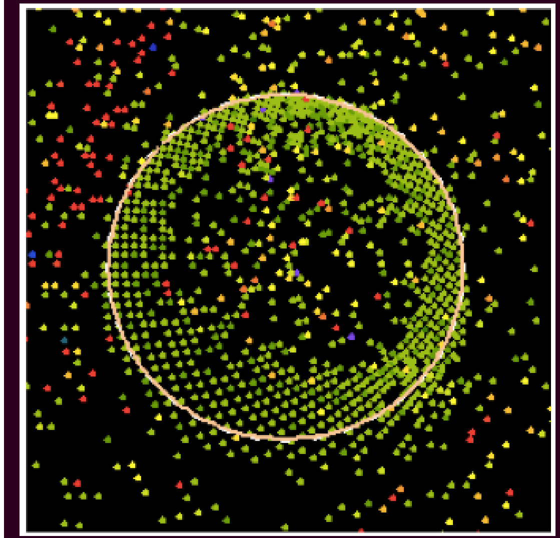

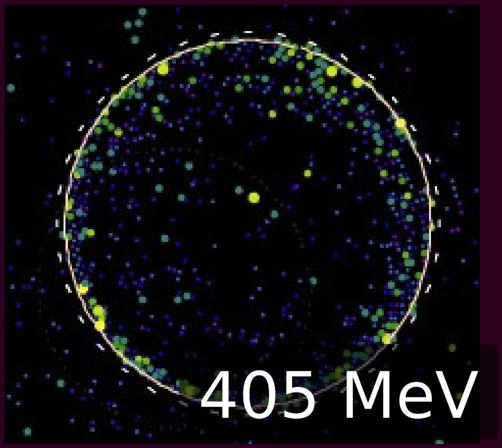

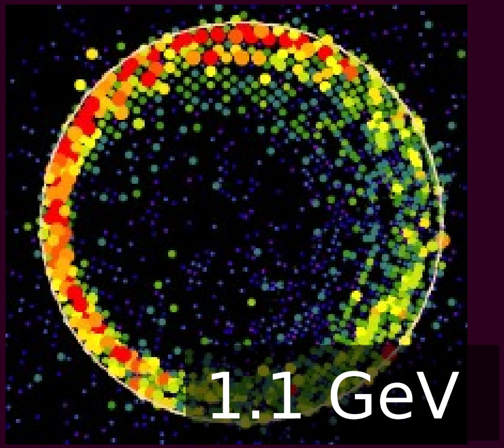

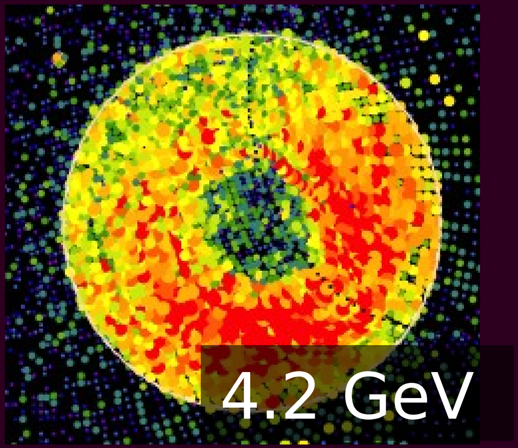

Data Samples

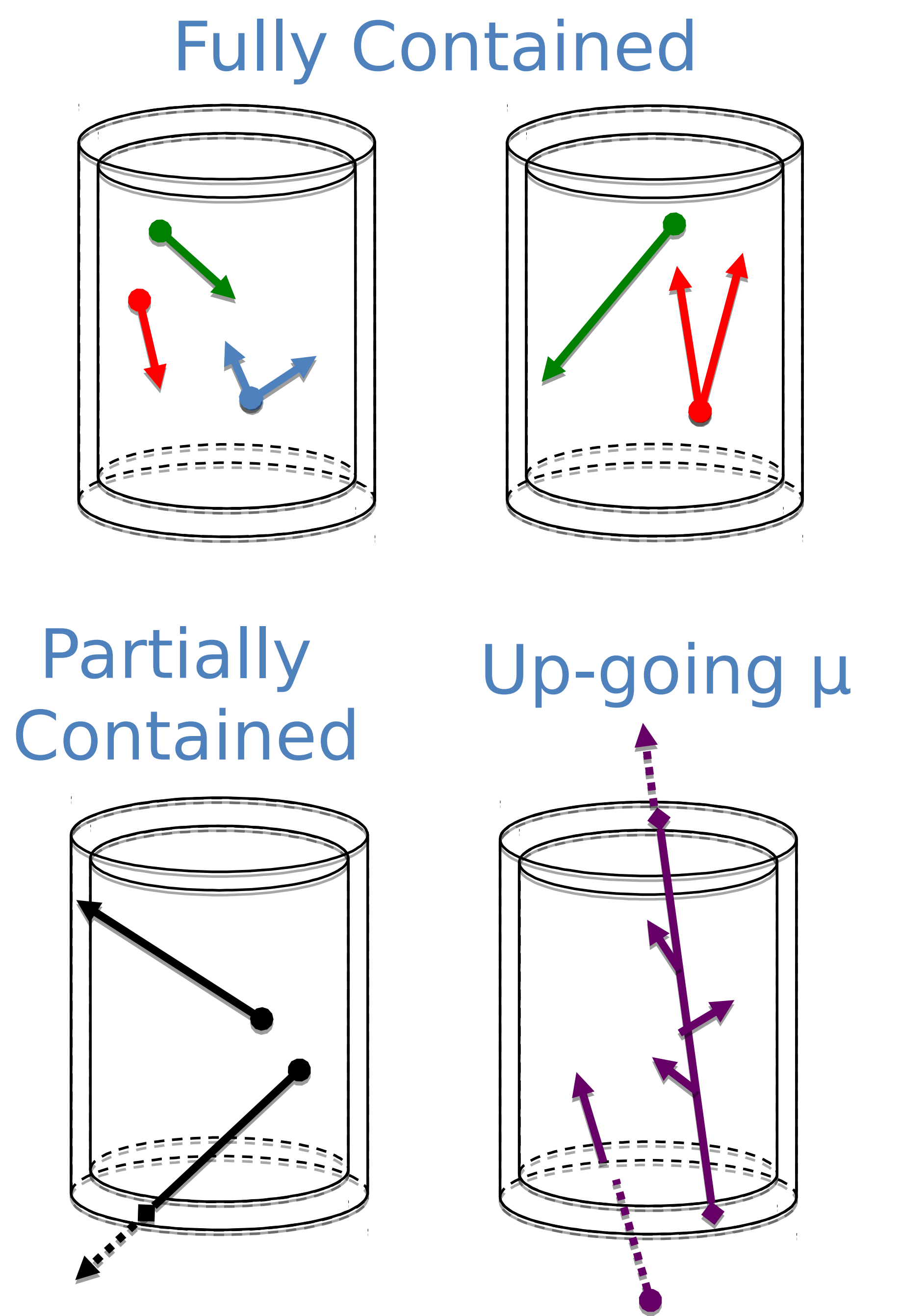

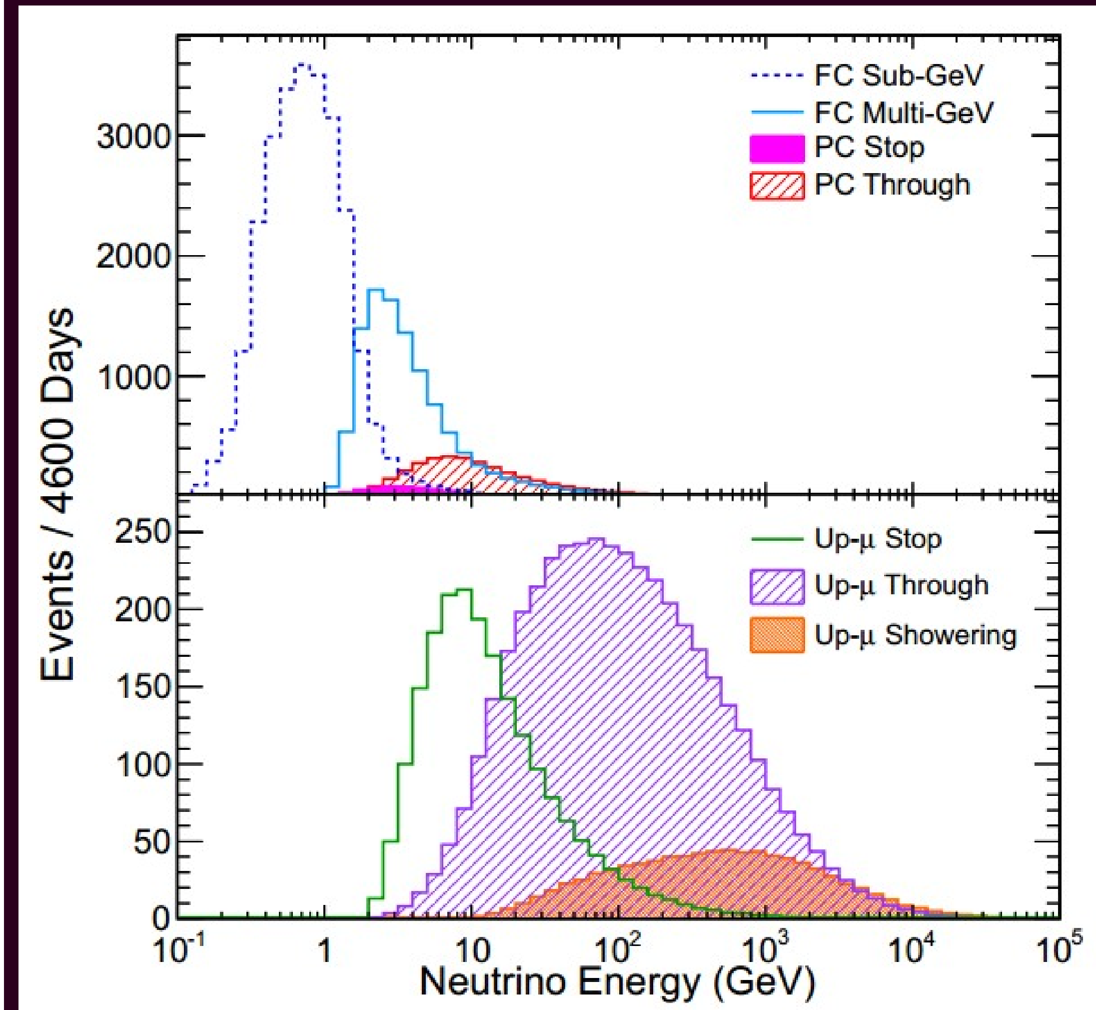

Sterile neutrino oscillation search

Introduction

- 4^{th} (5^{th}, 6^{th}...) neutrino mass state in the eV-scale may participate in neutrino oscillation.

$$U_{\text{PMNS}} = \begin{pmatrix} U_{e1} & U_{e2} & U_{e3} & U_{e4} \\ U_{\mu 1} & U_{\mu 2} & U_{\mu 3} & U_{\mu 4} \\ U_{\tau 1} & U_{\tau 2} & U_{\tau 3} & U_{\tau 4} \\ U_{s1} & U_{s2} & U_{s3} & U_{s4} \end{pmatrix}$$

- Assuming 1 sterile, there is significant tension in current measurements (LSND, MiniBooNE, radioactive source, reactor).

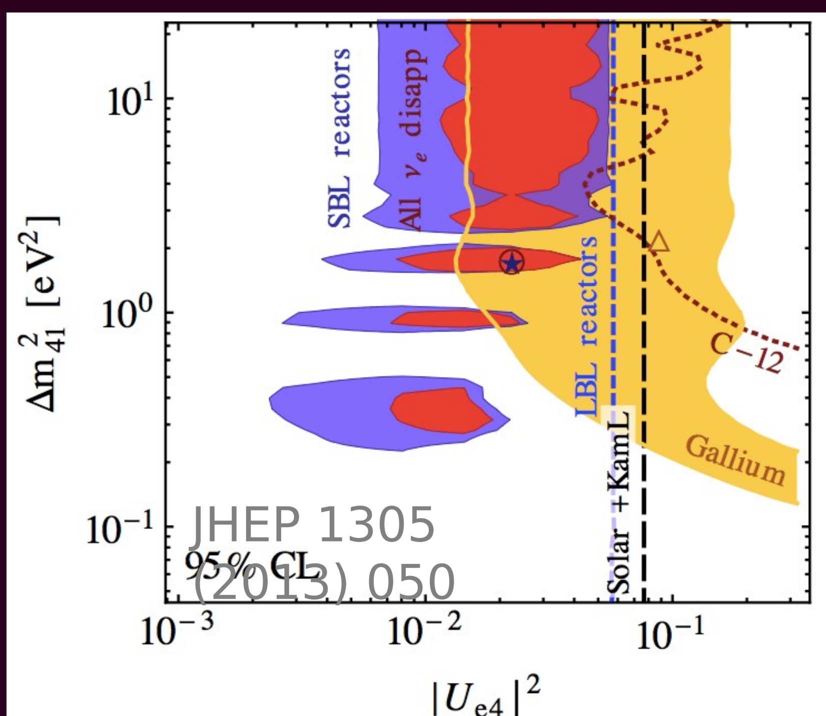

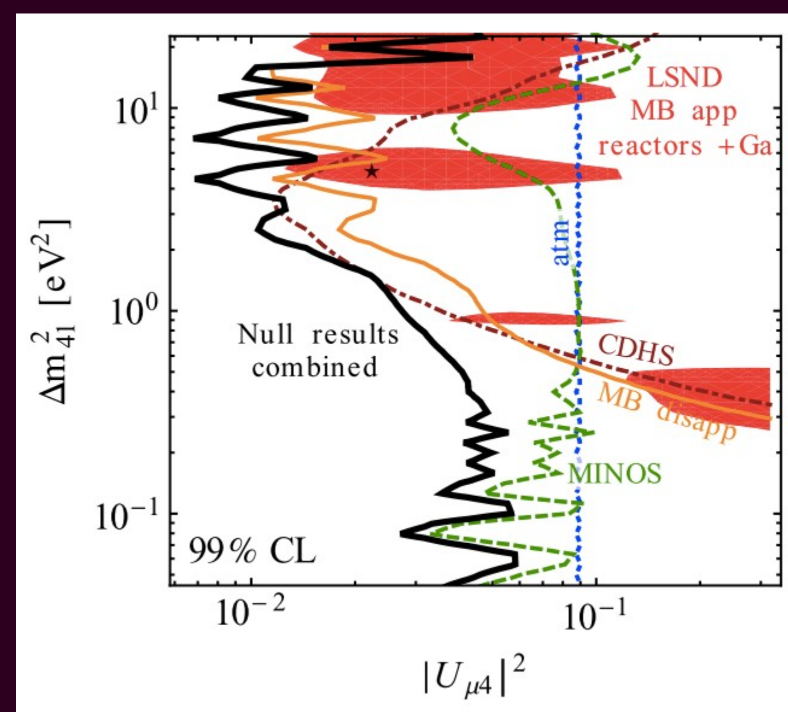

SK Approach

- Generally follow the approach in [1] with some simplifying assumptions for atmospheric sterile neutrinos.
  - Mass difference is large enough that oscillations are "fast", i.e. the sin(L / E) term can be approximated by a constant.
  - No ν_e-ν_s oscillations, i.e. $|U_{e4}| \sim 0$.
  - Complex phases are negligible.

- The validity of these assumptions is discussed in the backup.

- Firstly consider only 1 sterile, but in a way that can be easily extended at the end to *N* steriles (3+*N* neutrinos).

[1] M. Maltoni and T. Schwetz, Phys.Rev. D76, 093005 (2007)

SK Approach

- Some care must be taken with "sterile matter effects", e.g. the modified oscillation probabilities in the Earth:
  - ν_e has CC and NC interactions
  - ν_μ and ν_τ have only NC interactions
  - ν_s have no interactions
- Difficult computationally to calculate sterile and standard (ν_e) matter effects at the same time, so two fits are performed:

$$H = U M^{(3+N)} U^\dagger + V_e + V_s.$$

$$M^{(3+N)} = \frac{1}{2E}\mathrm{diag}\left(0, \Delta m^2_{21}, \ldots, \Delta m^2_{(3+N)1}\right),$$

$$V_e = \pm(G_F/\sqrt{2})\mathrm{diag}\,(2N_e, 0, \ldots)$$
$$V_s = \pm(G_F/\sqrt{2})\mathrm{diag}\,(0, 0, 0, N_n, N_n, \ldots)$$

No-ν_e Fit	Sterile Vacuum Fit
– Sterile matter effects – Fit for $\lvert U_{\tau 4}\rvert^2 + \lvert U_{\mu 4}\rvert^2$ – Over-constrains $\lvert U_{\mu 4}\rvert^2$	– ν_e matter effects – Fit for $\lvert U_{\mu 4}\rvert^2$ only – Most accurate $\lvert U_{\mu 4}\rvert^2$ limit, but no $\lvert U_{\tau 4}\rvert^2$ limit

No-ν_e Fit

Oscillation Probability

- The ν_μ survival probability in the no-ν_e approximation (3+1):

$$P_{\mu\mu} = \left(1 - |U_{\mu 4}|^2\right)^2 P^{(2)}_{\mu\mu} + |U_{\mu 4}|^4$$

$$H^{(2)} = H^{(2)}_{sm} + H^{(2)}_{s} :$$

$$= \frac{\Delta m^2_{31}}{4E} \begin{pmatrix} -\cos 2\theta_{23} & \sin 2\theta_{23} \\ \sin 2\theta_{23} & \cos 2\theta_{23} \end{pmatrix} \pm \frac{G_F N_n}{\sqrt{2}} \begin{pmatrix} |\tilde{U}_{s2}|^2 & \tilde{U}^*_{s2}\tilde{U}_{s3} \\ \tilde{U}_{s2}\tilde{U}^*_{s3} & |\tilde{U}_{s3}|^2 \end{pmatrix}$$

- $P^{(2)}$ represents the "standard" 2-flavour probability, plus the sterile matter effects
- U_{si} can be written in terms of $|U_{\tau 4}|^2$ and $|U_{\mu 4}|^2$ in a 3+1 framework.

No-ν_e Fit

$P(\nu_\mu$ to $\nu_\mu)$ Oscillogram

- Standard oscillation - **no sterile effects**

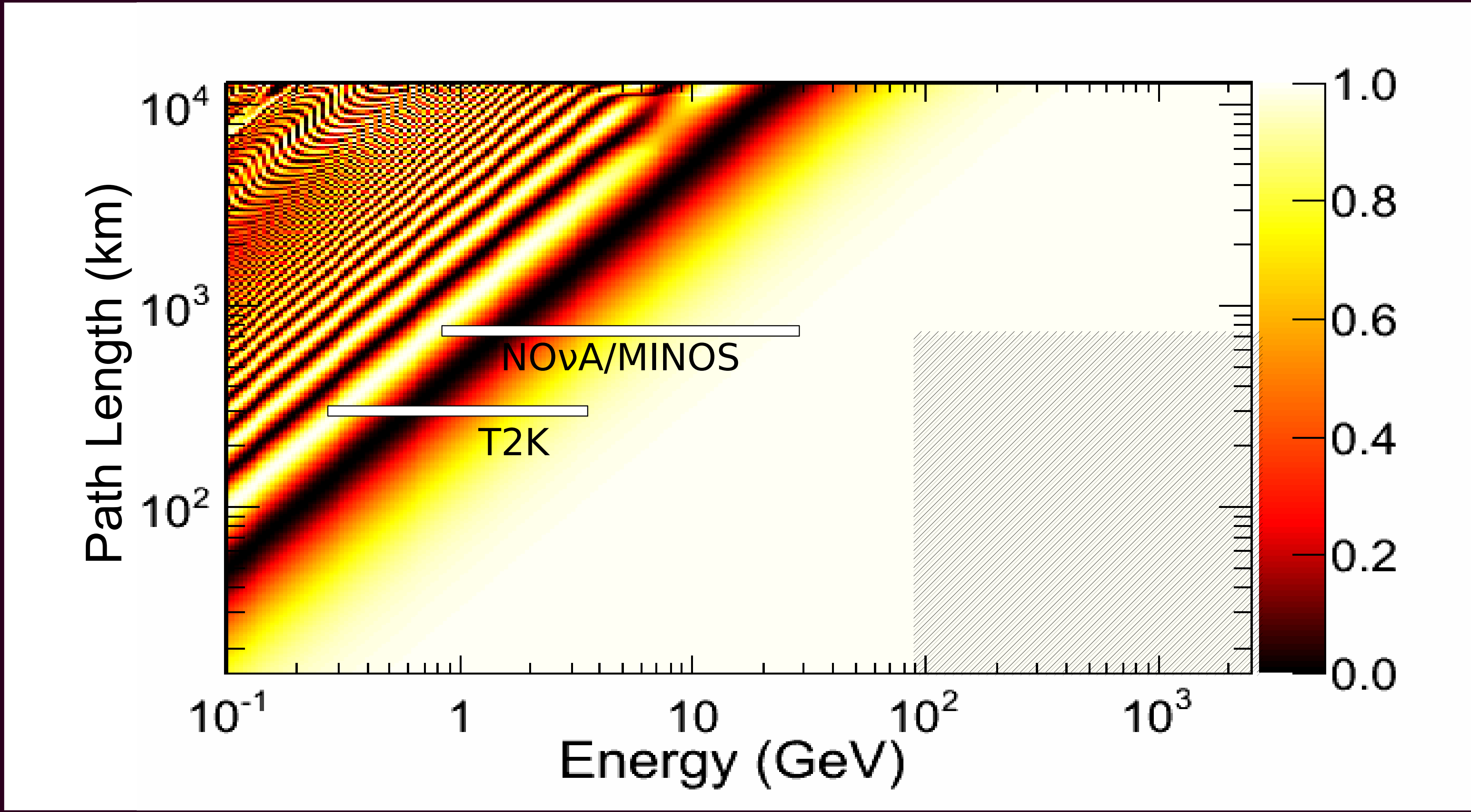

No-ν_e Fit

$P(\nu_\mu$ to $\nu_\mu)$ Oscillogram

- **With sterile effects**

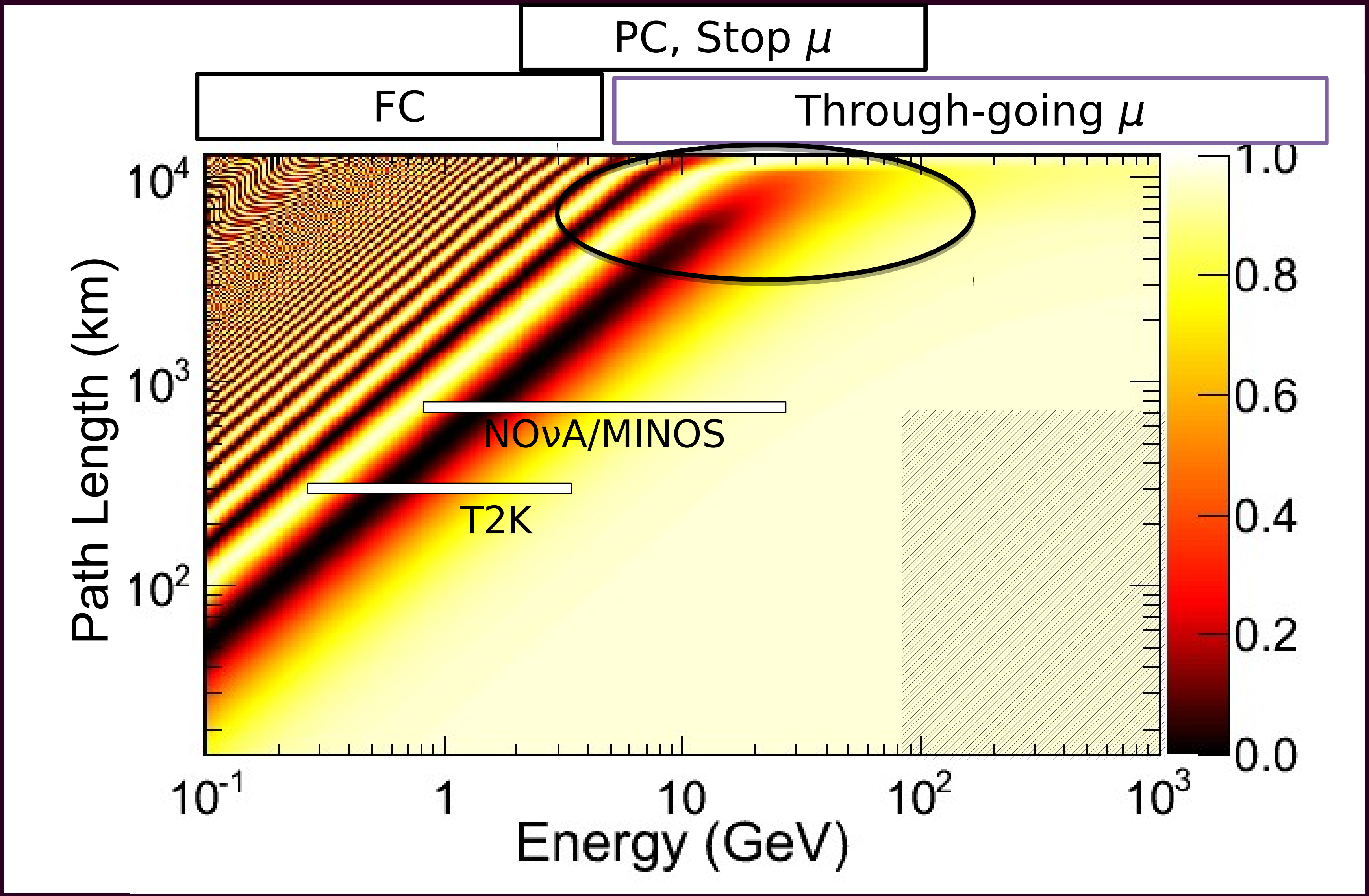

No-ν_e Fit

Fit Procedure

- Example distributions in some of the more sensitive samples.
- The fit procedure minimizes over all systematic errors to find the best fit for each hypothesis.
- Exclusion regions are found using the distance in $\Delta\chi^2$ to the best fit point, and difference in dimensionality of the parameter space (Wilks' theorem).

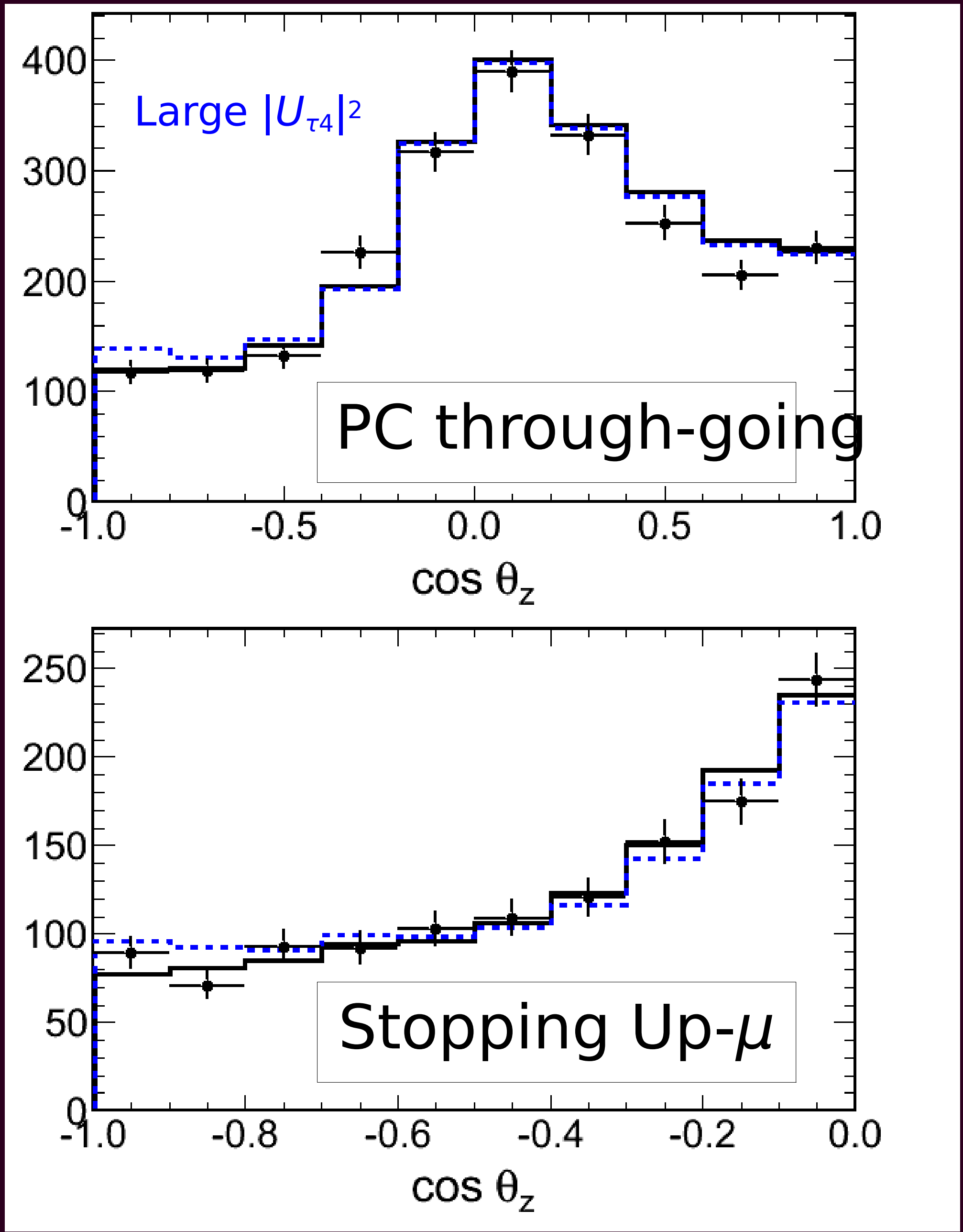

No-ν_e Fit

Results

Limit:
- 90 and 99% C.L. shown
- $|U_{\tau 4}|^2 < 0.23$ at 99% C.L.

Best fit at:
- $|U_{\tau 4}|^2 = 0.021$
- $|U_{\mu 4}|^2 = 0.012$

Goodness-of-fit:
$\chi^2/\text{dof} = 531.1/480\ (0.05)$

Favors ν_μ to ν_τ oscillations over ν_μ to ν_s oscillations.

The $|U_{\mu 4}|^2$ constraint is likely overestimated here.

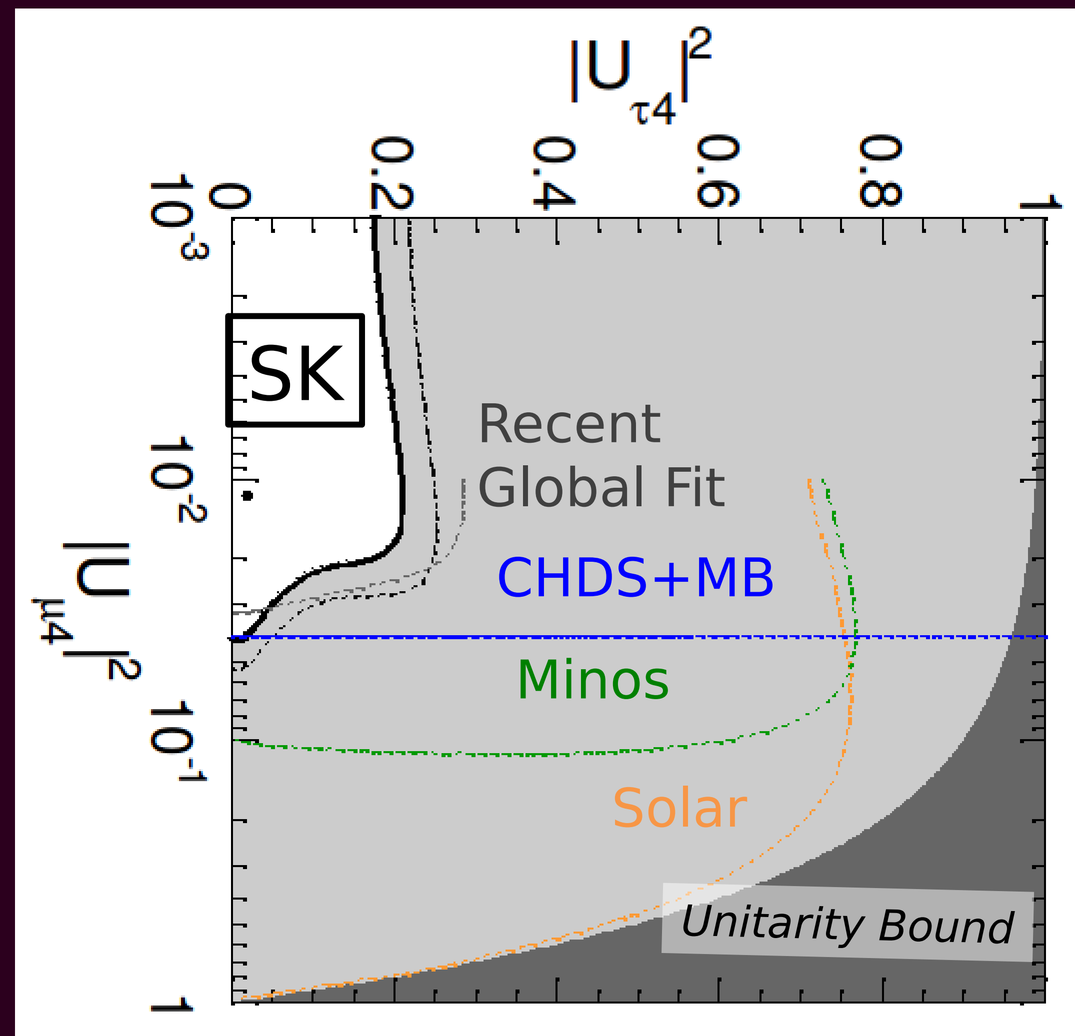

No-ν_e Fit

Extension to 3+N

- Matter term becomes

$$H^{(2)} = H_{\mathrm{SM}} \pm \underbrace{\frac{G_F N_n}{\sqrt{2}} \sum_\alpha \begin{pmatrix} |\tilde{U}_{\alpha 2}|^2 & \tilde{U}^*_{\alpha 2}\tilde{U}_{\alpha 3} \\ \tilde{U}_{\alpha 2}\tilde{U}^*_{\alpha 3} & |\tilde{U}_{\alpha 2}|^2 \end{pmatrix}}_{H_s(A_s,\,\theta_s)}$$

- Extend to multiple sterile neutrinos with a sum over sterile species α
- Because it is a 2-level system, any number of sterile parameters reduce to 3: A_s, θ_s, $|U_{\mu 4}|^2$
- We also make the results of this fit available in these parameters.

Sterile Vacuum Fit

Oscillation Probability

- The ν_μ survival probability in 3+1:

$$P_{\mu\mu} = \left(1 - |U_{\mu 4}|^2\right)^2 P_{\mu\mu}^{(3)} + |U_{\mu 4}|^4$$

- Here, $P^{(3)}$ is just the standard 3-flavor oscillation probability, including ν_e matter effects.
- Can't derive a limit for $|U_{\tau 4}|^2$
- No oscillogram - just a drop in normalization of all μ samples.
- Probability is not unique at each L/E due to matter effects being dependent on L and E individually.

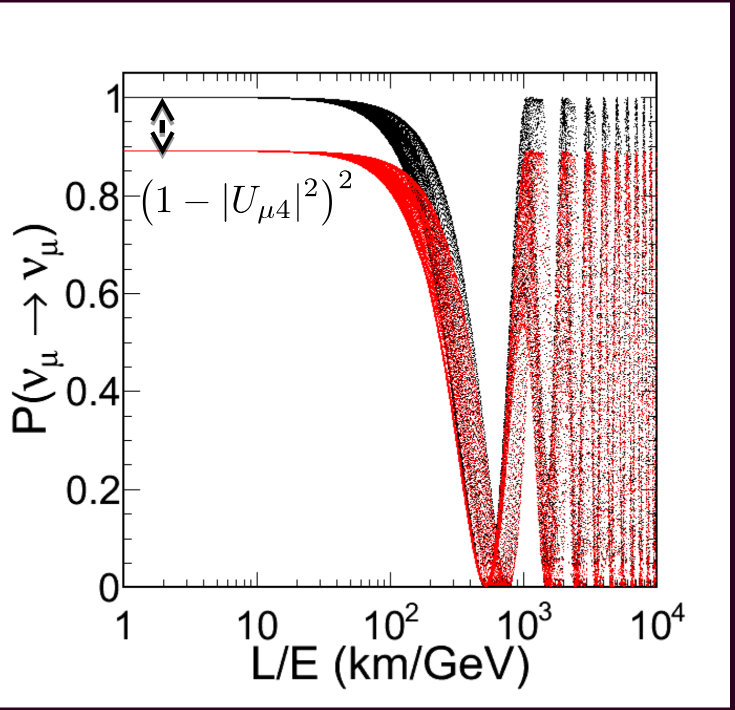

Sterile Vacuum Fit

Fit Procedure

- Fit is then essentially systematics-limited.
  - The normalization of the *e* samples are used to constrain the normalization of the μ samples more accurately.
- Best fit $|U_{\mu 4}|^2 = 0.016$
  - Figure shows the best fit including minimization over systematics (red line), and the same sterile parameters without shifting the systematics (red dotted).

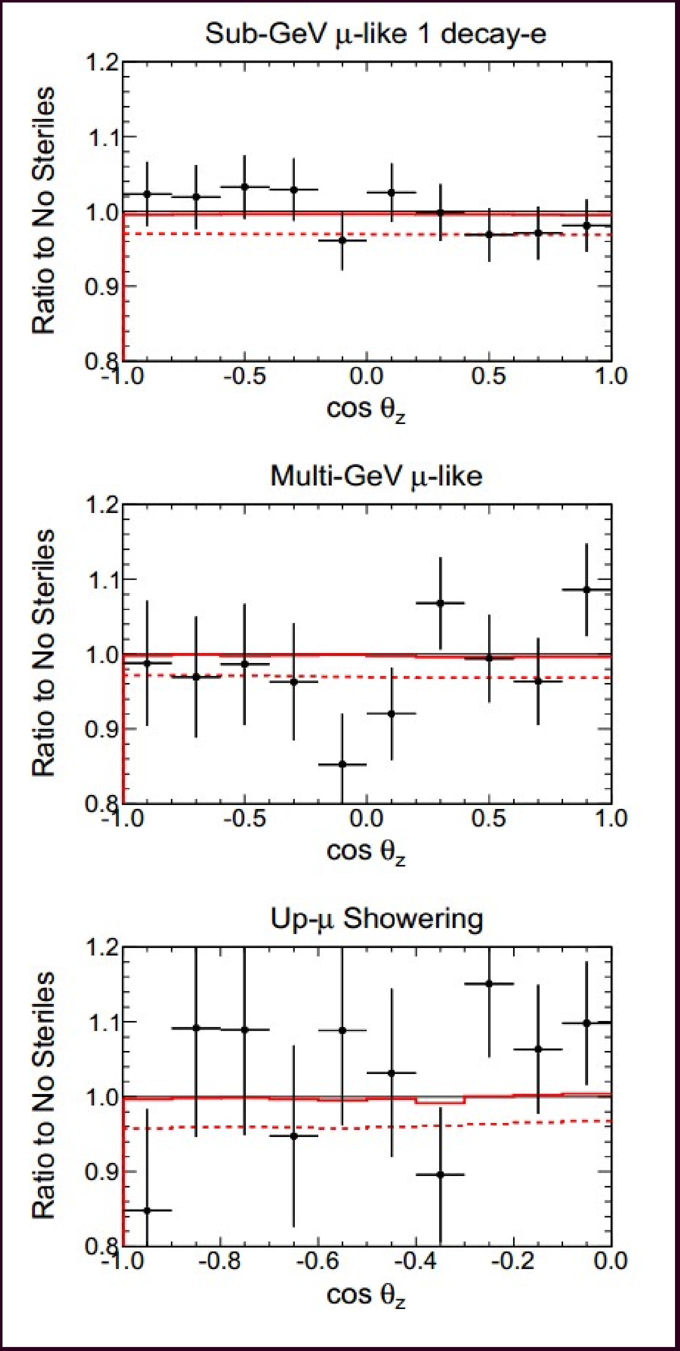

Sterile Vacuum Fit

Results

Best fit: $|U_{\mu 4}|^2 = 0.016$

$|U_{\mu 4}|^2 < 0.041$ at 90% C.L.

$|U_{\mu 4}|^2 < 0.054$ at 99% C.L.

Sensitivity: 0.024 at 90%

- No strong sterile-driven ν_μ disappearance.
- $\Delta\chi^2$ of 1.1 between the best fit and no sterile neutrinos.
- Analysis is systematics limited.

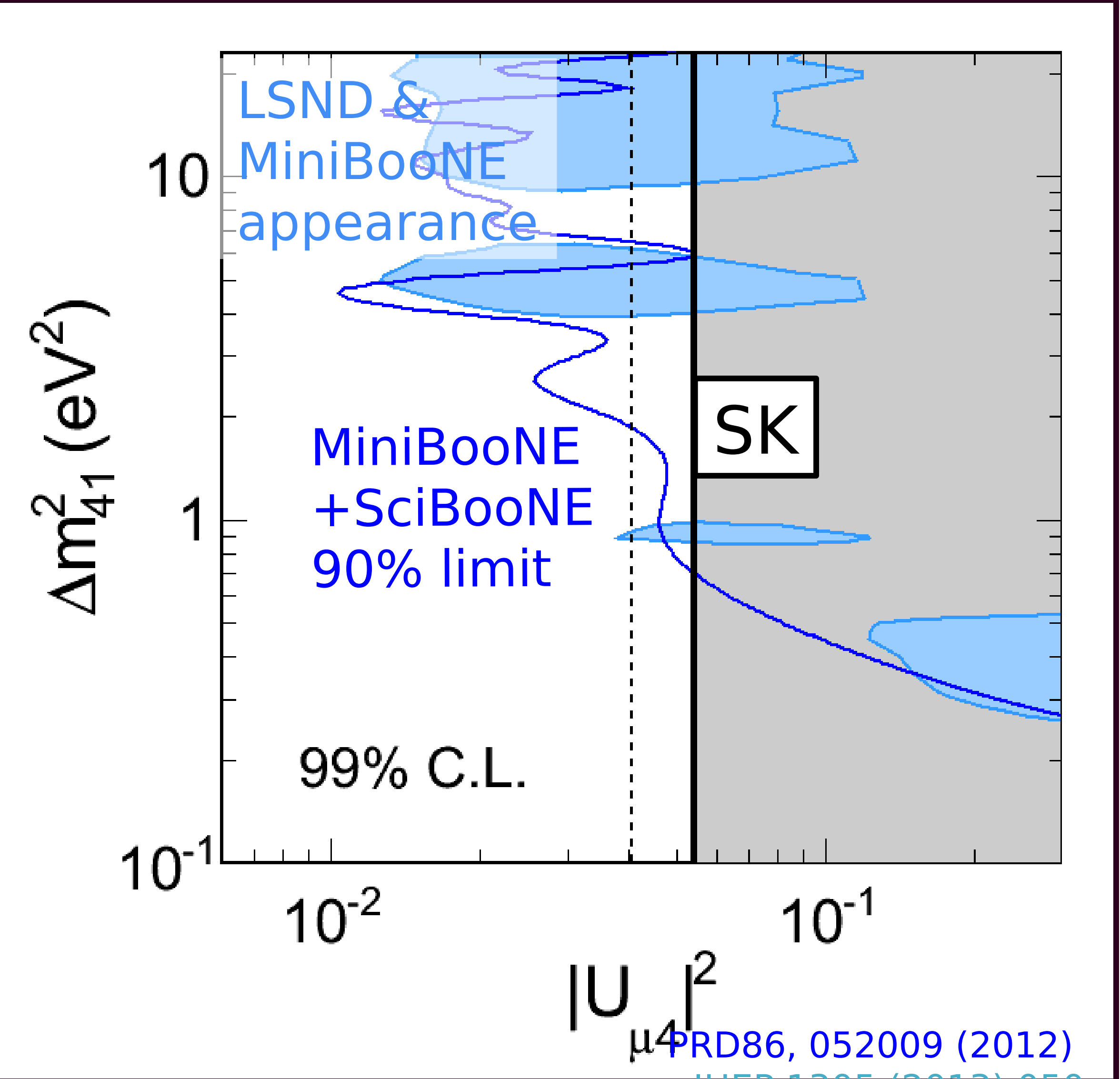

PRD86, 052009 (2012)
JHEP 1305 (2013) 050

Sterile Vacuum Fit

Extension to 3+N

- The ν_μ survival probability in 3+N:

$$P_{\mu\mu} = \left(1 - d_\mu^2\right)^2 P_{\mu\mu}^{(3)} + \sum_\alpha |U_{\alpha 4}|^4$$

$$d_\mu = \sum_\alpha |U_{\alpha 4}|^2$$

- Very similar to the 3+1 formula with $|U_{\mu 4}|^2 \rightarrow d_\mu$

MeV sterile decay search

“Heavy” Sterile Neutrinos

- A state $m_4 \gtrsim \mathrm{keV}$ is separated from the oscillation effects.
- The phenomenology varies depending on the mass, and in some cases we may have observable decay products.
  - For example, take $m_4 \sim MeV$
    - Motivated by e.g. νMSM - standard Seesaw mechanism, but Majorana masses M_I are chosen below electroweak scale.

MeV Sterile Decay

- Considering $10 \lesssim m_4 \lesssim 100\ \mathrm{MeV}$, a heavy neutrino ν_4 that mixes with ν_μ may be produced in atmosphere by μ , K , or π decay.
  - We consider only the mixing parameter $|U_{\mu 4}|^2$ as electron-mixing is already excluded at 2~3 orders of magnitude lower in this region, and atmospheric decay has negligible τ component.
  - Visible decay products, for example Super-Kamiokande can see the decay below, with two electron-like Čerenkov rings.

Cosmic ray

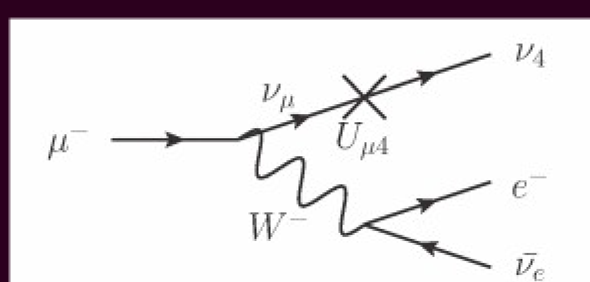

Atmosphere

SK

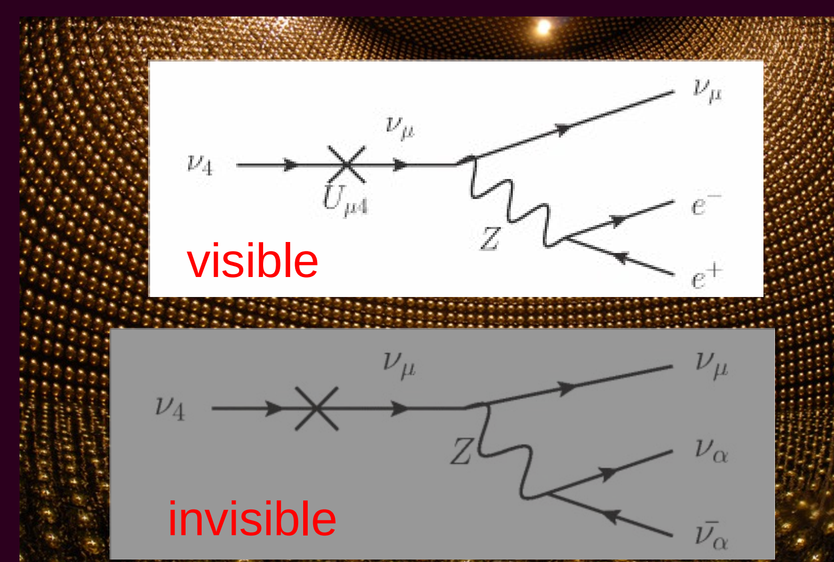

Sterile Simulation

- Using Honda-flux atmospheric MC, events are reweighted by "sterile creation probability", e.g. for muon decay:

$$\frac{\Gamma(\mu^- \to e^-\nu_e\nu_4)}{\Gamma(\mu^- \to e^-\nu_e\nu_\mu)} = |U_{\mu 4}|^2(1 - 8r + 8r^3 - r^4 - 24r^2\ln(r)) \qquad r = \left(\frac{m_4}{m_\mu}\right)^2$$

  - Neutrinos from pion and kaon decays also reweighted.

- Then track event probability to decay inside of SK.
  - Path-length dependency
    = zenith angle dependency

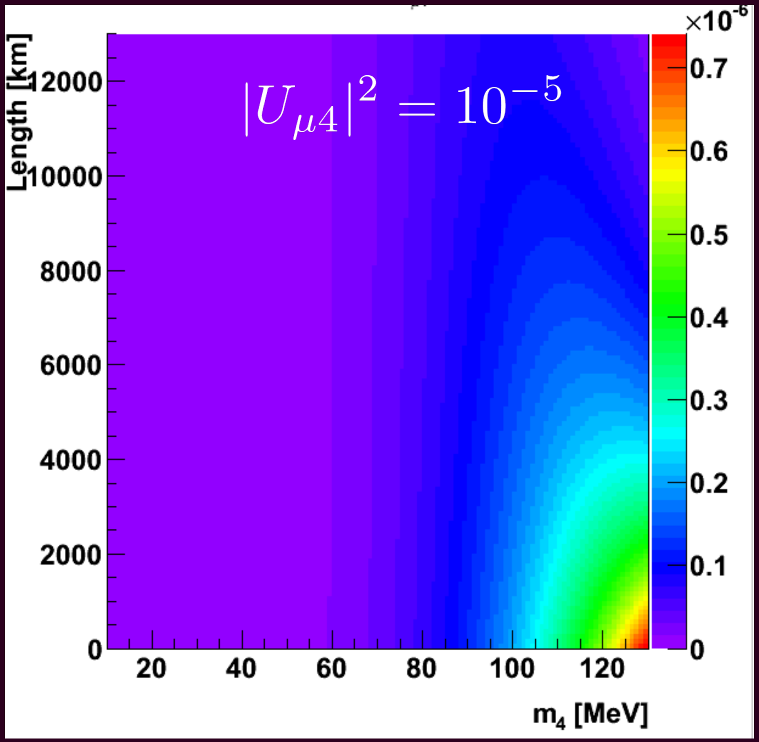

Fit Method

- The visible decay is a 3-body decay ($e+$, $e-$, ν_μ) so we should see a signal distribution (not peak) in the invariant mass distribution of the e-like two-ring event sample.
  - Figure shows MC truth.

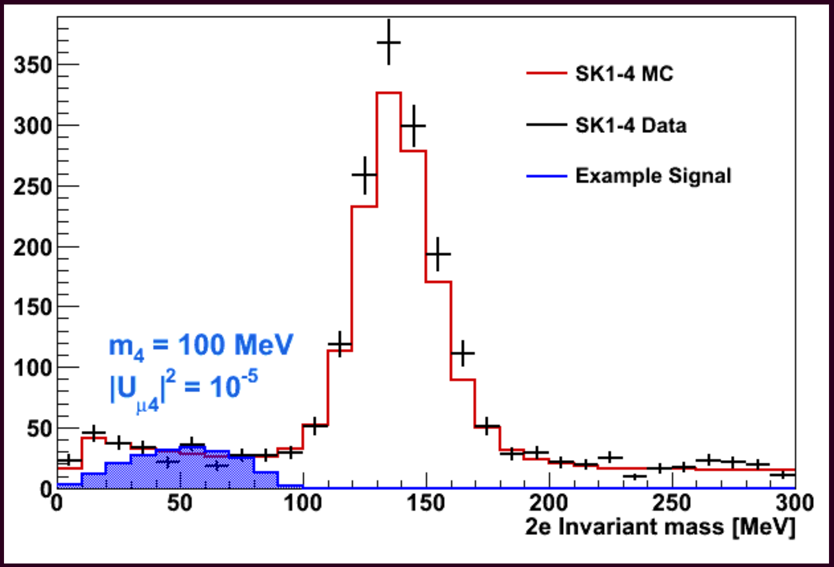

- So we see signal in **e+ e- invariant mass** and **zenith angle**.

Background

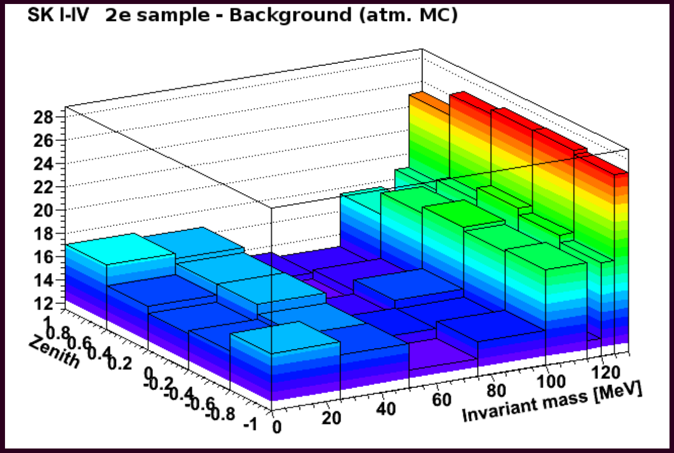

Signal

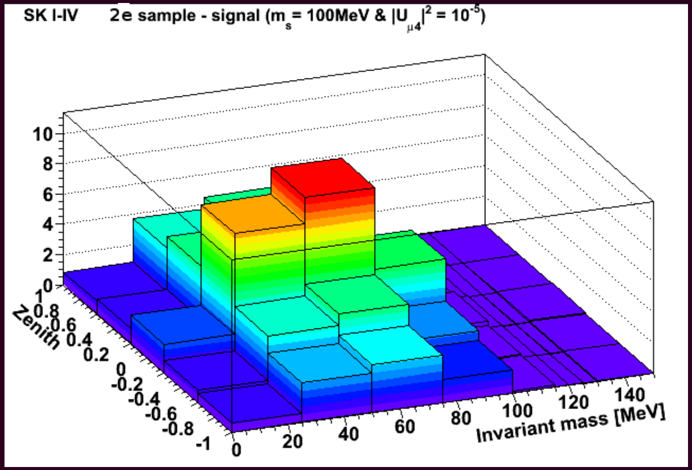

- Fit procedure similar to oscillation case (minimizing over systematics).

Results

- Compared to SK study by T. Asaka, our internal SK study uses the Honda-flux prediction and full knowledge of the detector and data-set. Contribution to steriles from Kaon-decay is also estimated.
- The final extracted limit is still below CERN PS191.
- There are some easy extensions to the phenomenology for higher masses ~ 400 MeV.
- Depending on the mass region, need to consider phenomenology more, but SK (and especially HK) may have some good search power regions.

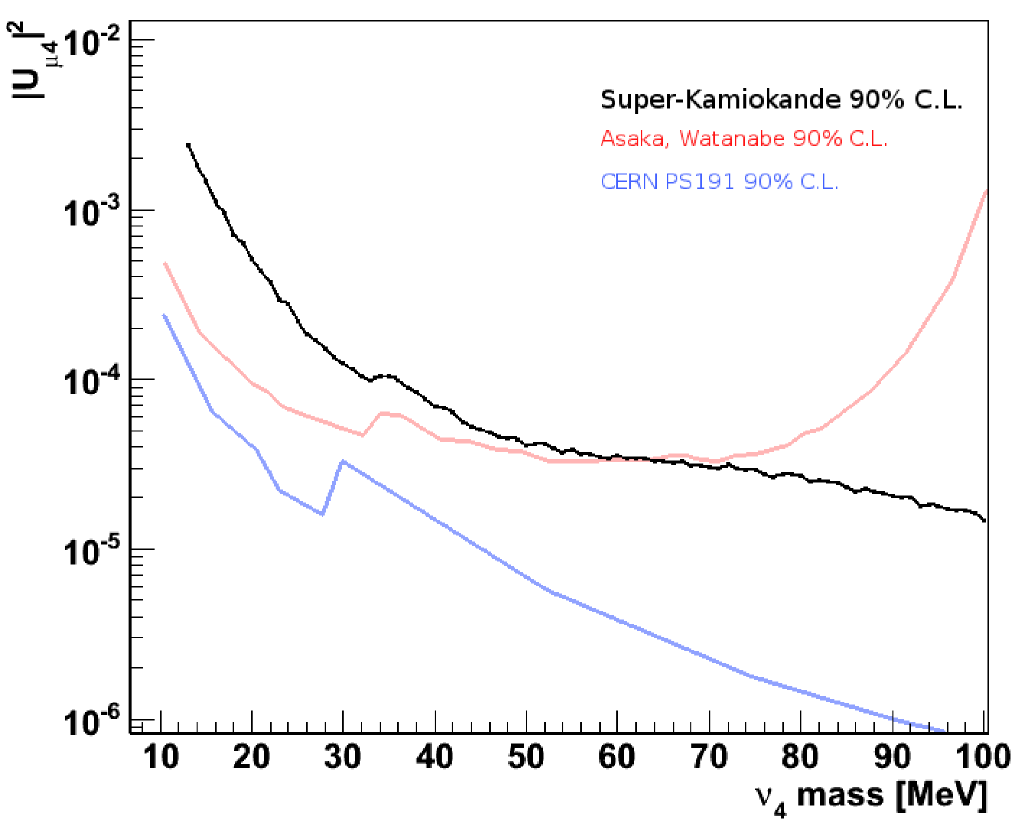

Non Standard Neutrino Interactions

NSI - Introduction

- A very general model for non-standard neutrino interactions (NSI) with matter can be introduced with the Hamiltonian

$$H_{\alpha\beta} = \frac{1}{2E} U_{\alpha j} \begin{pmatrix} 0 & 0 & 0 \\ 0 & \Delta m_{21}^2 & 0 \\ 0 & 0 & \Delta m_{31}^2 \end{pmatrix} (U^\dagger)_{k\beta} + V_{\mathrm{MSW}} + \sqrt{2} G_F N_f(\vec{r}) \begin{pmatrix} \varepsilon_{ee} & \varepsilon_{e\mu}^* & \varepsilon_{e\tau}^* \\ \varepsilon_{e\mu} & \varepsilon_{\mu\mu} & \varepsilon_{\mu\tau}^* \\ \varepsilon_{e\tau} & \varepsilon_{\mu\tau} & \varepsilon_{\tau\tau} \end{pmatrix}$$

  which represents respectively: the standard neutrino oscillation, the standard matter effect, and the NSI; for a flavour change $\nu_\alpha \rightarrow \nu_\beta$.

- The NSI matrix includes
  - Flavour Changing Neutral Current (FCNC, the off-diagonal ε_{xy}).

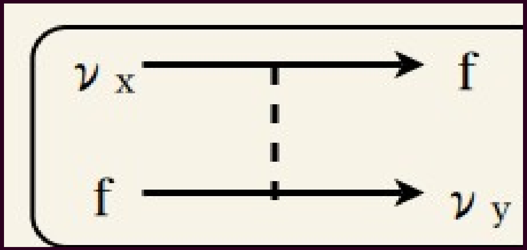

  - Lepton Non-Universality (NU, the on-diagonal ε_{xx}).

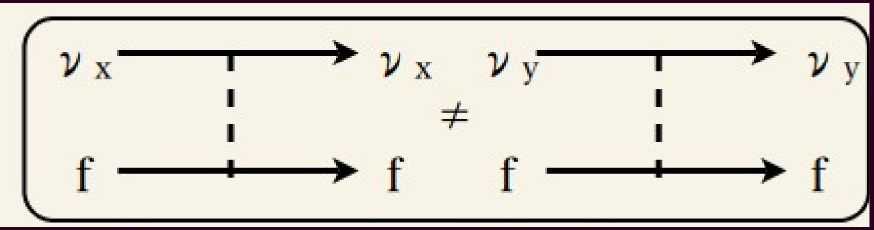

- Motivations from R-parity violating SUSY, neutral heavy leptons...

SK Search

- Two methods are adopted that can simultaneously test NSI and neutrino oscillation in the atmospheric data.

- Two-flavour approach
  - NSI coexists with the dominant $\nu_\mu \leftrightarrow \nu_\tau$ atmospheric oscillations.
  - ν_e is completely decoupled and ignored (no MSW effect).
    - Constrains $\varepsilon_{\mu\mu}$, $\varepsilon_{\mu\tau}$, and $\varepsilon_{\tau\tau}$.

- Three-flavour "hybrid" approach
  - $\nu_\mu \leftrightarrow \nu_\tau$ atmospheric oscillations and $\nu_e \leftrightarrow \nu_\tau$ NSI.
    - Constrains ε_{ee}, $\varepsilon_{e\tau}$, and $\varepsilon_{\tau\tau}$.

Two-Flavour approach

- Following [2], assuming NSI is dominated by d-quark interactions, we define $\varepsilon = \varepsilon_{\mu\tau}$ (FCNC part) and $\varepsilon' = \varepsilon_{\tau\tau} - \varepsilon_{\mu\mu}$ (NU part).
- Survival probability is somewhat complicated (backup), but we have an effective mixing angle *Θ* and oscillation wavelength correction factor *R*, which are dependent on ε, ε' and the neutrino energy *E*.

$$P_{\nu_\mu \to \nu_\mu} = 1 - P_{\nu_\mu \to \nu_\tau} = 1 - \sin^2 2\Theta \sin^2 \left(\frac{\Delta m^2_{23} L}{4E} R \right)$$

- Predicted effect thus in different samples for ε (FCNC) and ε' (NU):

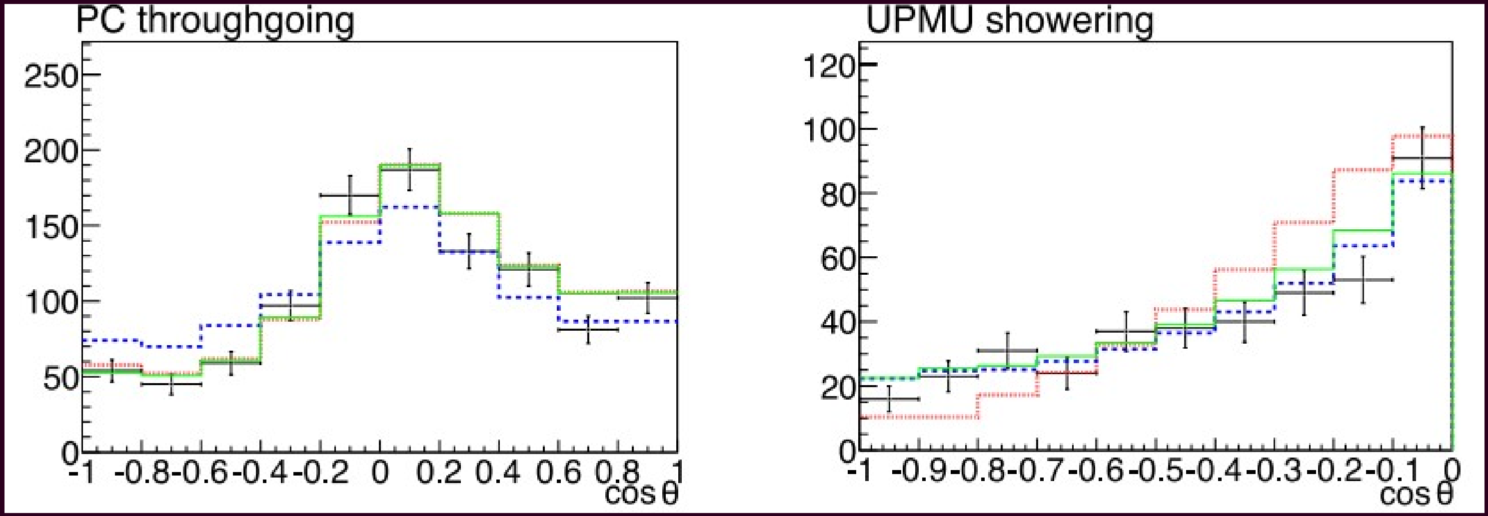

[2] M. C. Gonzalez-Garcia and M. Maltoni Phys. Rev. D 70, 033010 (2004)

Two-flavour Results

- Best fit information:

$$\sin^2 2\theta_{23} = 1.00, \quad \Delta m^2_{23} = 2.2 \times 10^{-3}\mathrm{eV}^2,$$
$$\varepsilon = 1.0 \times 10^{-3}, \quad \varepsilon' = -2.7 \times 10^{-2}$$
$$\chi^2_{min} = 838.9 \ / \ 746.0 \text{ d.o.f.}$$

- ε (FCNC) limits are tighter compared to other experiments, while ε' (NU) limits are not quite as strong.

ε' = +1

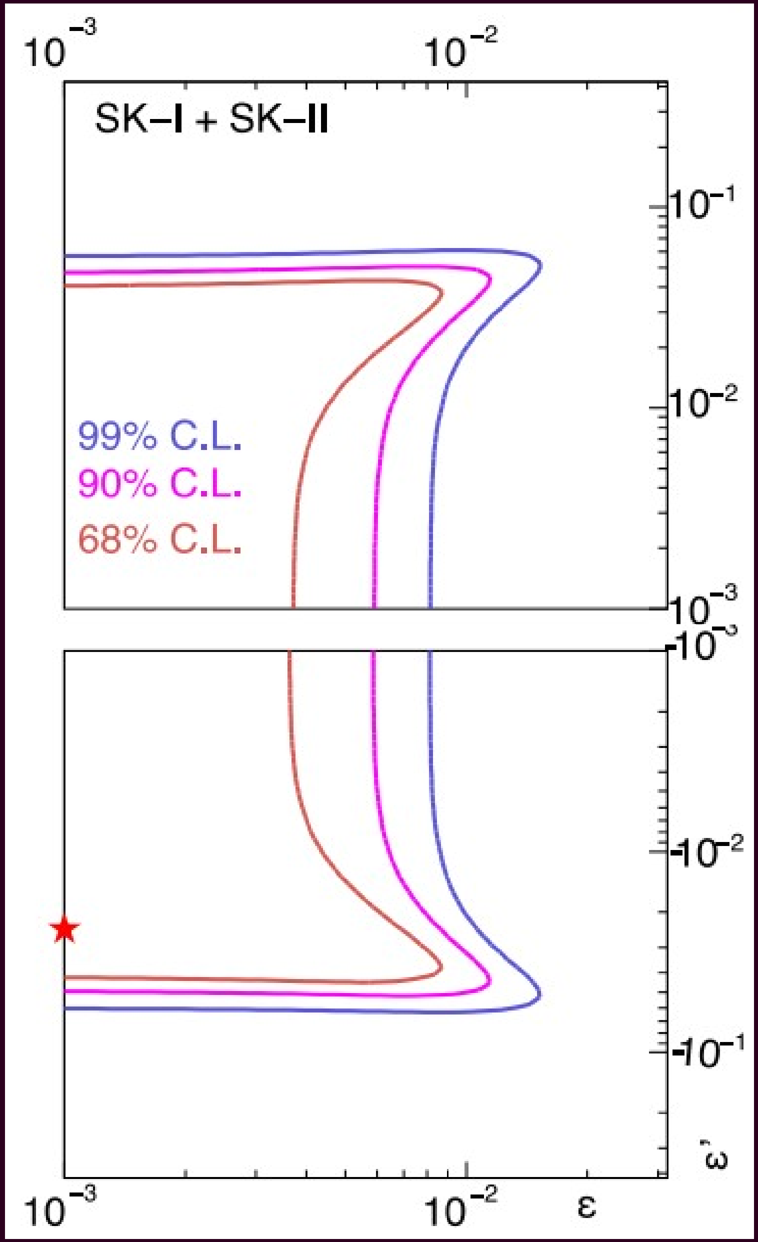

ε' = -1

Three-Flavour approach

- In the three-flavour case, the effective Hamiltonian becomes

$$H_{\text{hybrid}} = \underbrace{\boxed{\frac{1}{2E} U_{\alpha j} \begin{pmatrix} 0 & 0 & 0 \\ 0 & 0 & 0 \\ 0 & 0 & \Delta m^2_{31} \end{pmatrix}_{jk} (U)^{\dagger}_{k\beta}}}_{\text{vacuum term}} + \underbrace{\boxed{V_{MSW} + \sqrt{2} G_F N_f \begin{pmatrix} \varepsilon_{ee} & 0 & \varepsilon_{e\tau} \\ 0 & 0 & 0 \\ \varepsilon^{\star}_{e\tau} & 0 & \varepsilon_{\tau\tau} \end{pmatrix}}}_{\text{matter term}}$$

- One drawback of this model is that as $\varepsilon_{e\tau} \rightarrow 0$, eigenstates revert back to the vacuuum ones, and there is no ability to constrain ε_{ee}.

- Example distributions: $\varepsilon_{ee}=0$, $\varepsilon_{e\tau}=0$, $\varepsilon_{\tau\tau}=0$ and $\varepsilon_{ee}=0$, $\varepsilon_{e\tau}=0.2$, $\varepsilon_{\tau\tau}=0.2$

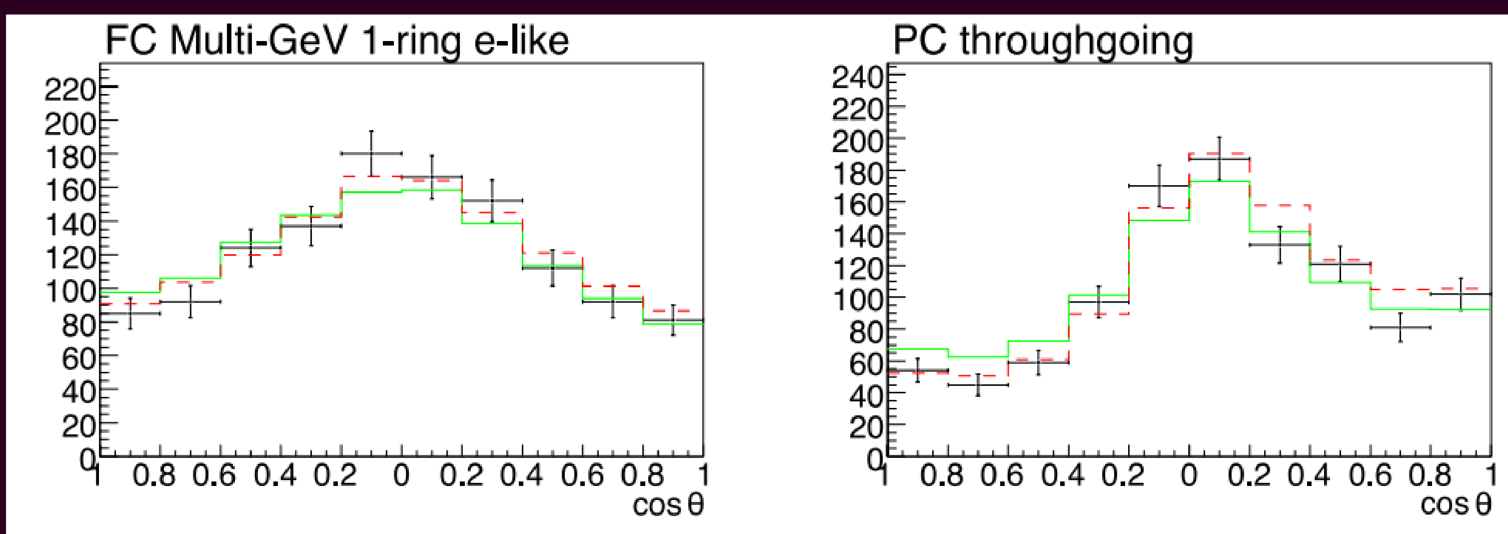

Three-Flavour Results

- Results given at fixed ε_{ee} for $\varepsilon_{e\tau}$ and $\varepsilon_{\tau\tau}$, θ_{23} and Δm^2_{23} integrated out.

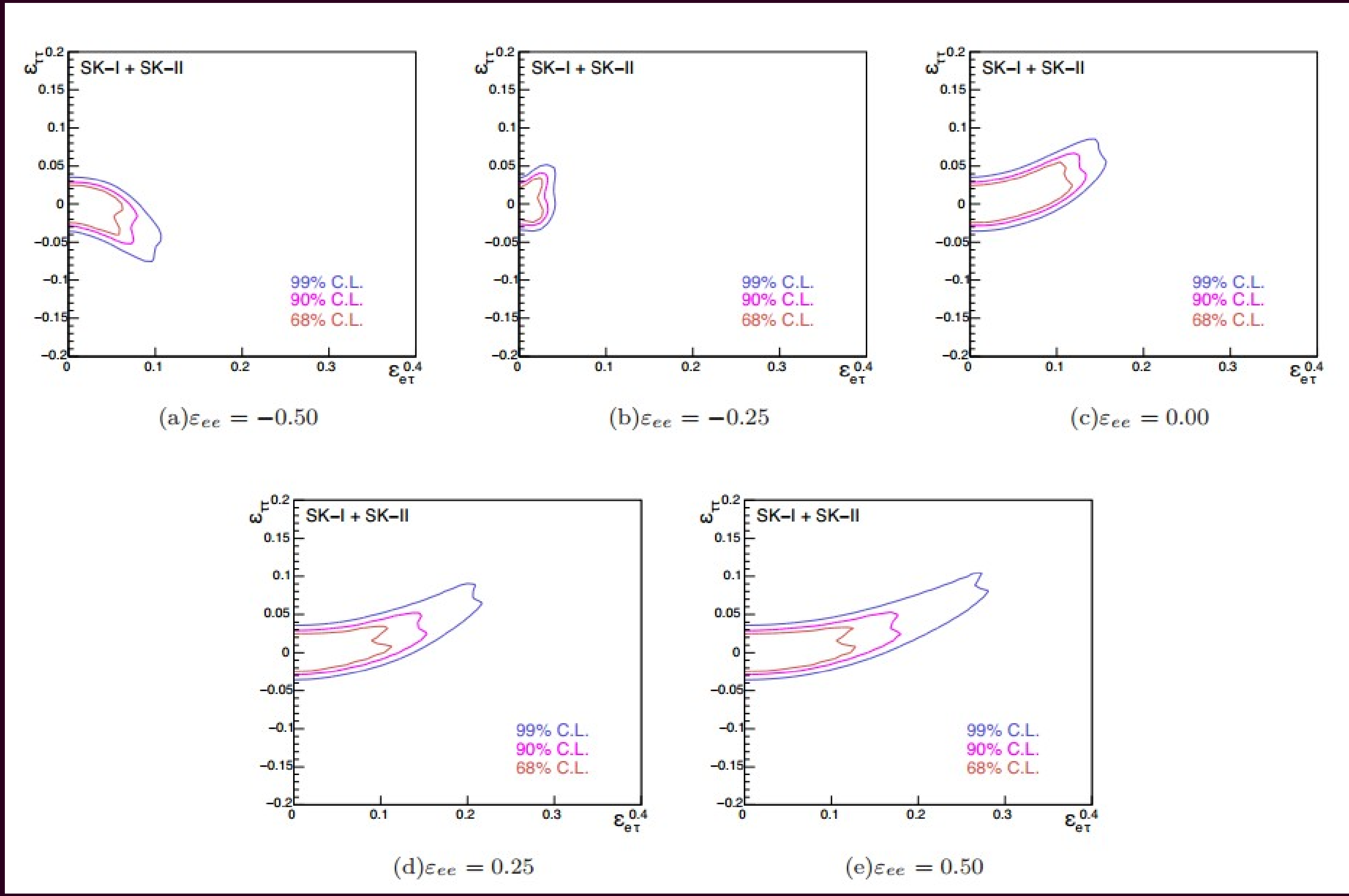

(a) $\varepsilon_{ee} = -0.50$ (b) $\varepsilon_{ee} = -0.25$ (c) $\varepsilon_{ee} = 0.00$ (d) $\varepsilon_{ee} = 0.25$ (e) $\varepsilon_{ee} = 0.50$

- Modern values of θ_{13} and the SK III-IV dataset should result in some improvements of these constraints.

Lorentz Invariance Violation search

Introduction

- Violations of Lorentz invariance are predicted at the Planck scale by a variety of models, such as space-time foam interactions.
- The Standard Model Extension (SME) adds to the Standard Model all possible Lorentz-Violating (LV) terms.
  - Terms may be directional (indicating a preferred spatial direction) or isotropic.
  - Neutrino oscillations are a sensitive probe of these coefficients.
    - In this analysis, we focus on isotropic coefficients (effects relating to L and E).

Coefficient	Unit	d	CPT	Oscillation Effect
Isotropic				
$a^T_{\alpha\beta}$	GeV	3	odd	$\propto L$
$c^{TT}_{\alpha\beta}$	-	4	even	$\propto LE$
Directional				
$a^X_{\alpha\beta}, a^Y_{\alpha\beta}, a^Z_{\alpha\beta}$	GeV	3	odd	sidereal variation
$c^{XX}_{\alpha\beta}, c^{YZ}_{\alpha\beta}, \ldots$	-	4	even	sidereal variation

TABLE I. Lorentz-violating coefficients and their properties. The last row includes all possible combinations of X, Y, Z, and T except TT. d refers to the dimension of the operator. α and β range over the neutrino flavors, e, μ, and τ. The X, Y, and Z indicate coefficients which introduce effects in a particular direction in a Lorentz-violating preferred reference frame. The T and TT terms are not associated with any direction and thus introduce isotropic distortions in the oscillation pattern.

Oscillations

- The neutrino Hamiltonian (3-flavour oscillation, matter and LV terms):

$$H = U \begin{pmatrix} 0 & 0 & 0 \\ 0 & \frac{\Delta m^2_{21}}{2E} & 0 \\ 0 & 0 & \frac{\Delta m^2_{31}}{2E} \end{pmatrix} U^\dagger \pm \sqrt{2} G_F \begin{pmatrix} N_e & 0 & 0 \\ 0 & 0 & 0 \\ 0 & 0 & 0 \end{pmatrix} \pm \begin{pmatrix} 0 & a^T_{e\mu} & a^T_{e\tau} \\ \left(a^T_{e\mu}\right)^* & 0 & a^T_{\mu\tau} \\ \left(a^T_{e\tau}\right)^* & \left(a^T_{\mu\tau}\right)^* & 0 \end{pmatrix} - E \begin{pmatrix} 0 & c^{TT}_{e\mu} & c^{TT}_{e\tau} \\ \left(c^{TT}_{e\mu}\right)^* & 0 & c^{TT}_{\mu\tau} \\ \left(c^{TT}_{e\tau}\right)^* & \left(c^{TT}_{\mu\tau}\right)^* & 0 \end{pmatrix}$$

  - Unlike NSI, the new terms are not matter effects.
  - Diagonal terms cannot be observed.

- Perturbation method on the Hamiltonian was found to be inappropriate over the large range of L and E in the SK dataset.
  - First analysis to use the exact diagonalization of *H.*

$P(\nu_\mu \to \nu_\mu)$ Oscillations

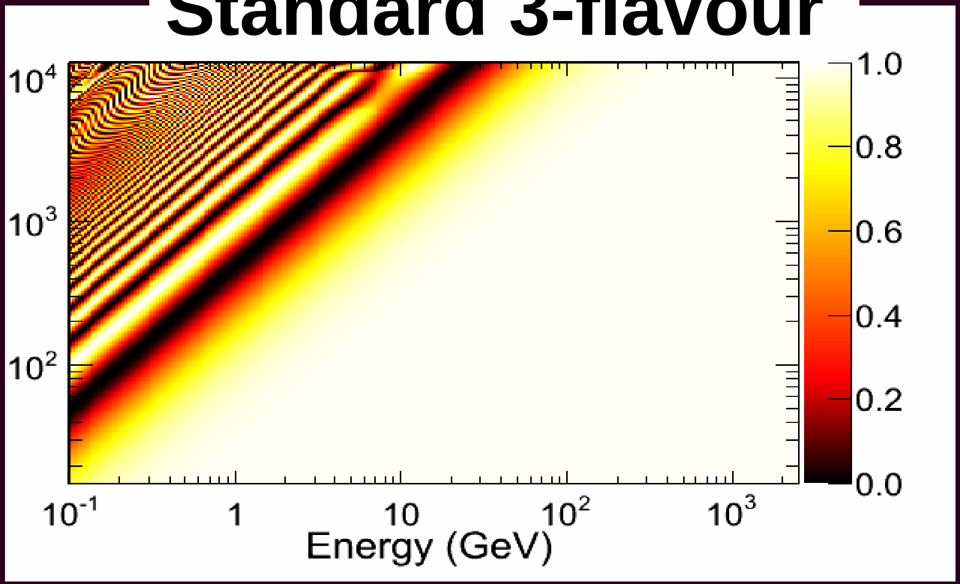

$\mathrm{Re}\, a^{T}_{\mu\tau}$ = 10^{-22}

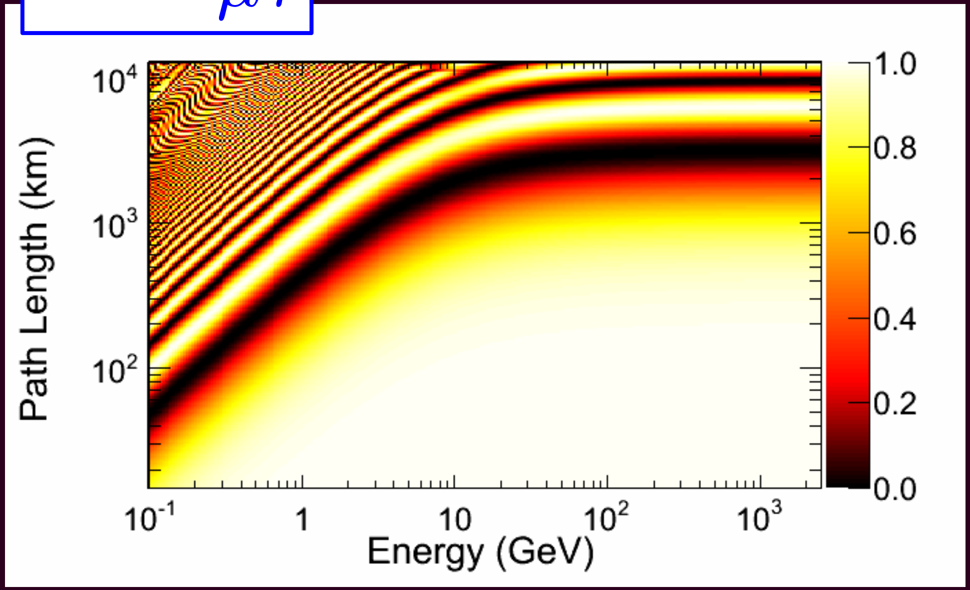

$\mathrm{Re}\, c^{TT}_{\mu\tau}$ = 10^{-22}

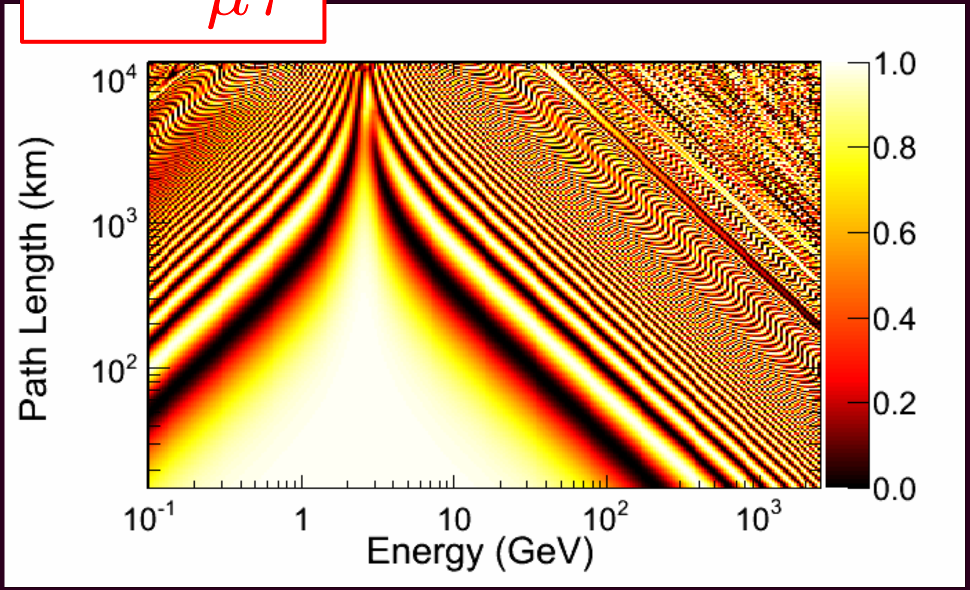

Sensitive Samples

$\mathrm{Re}\, a^{T}_{\mu\tau}$ $\mathrm{Re}\, c^{TT}_{\mu\tau}$

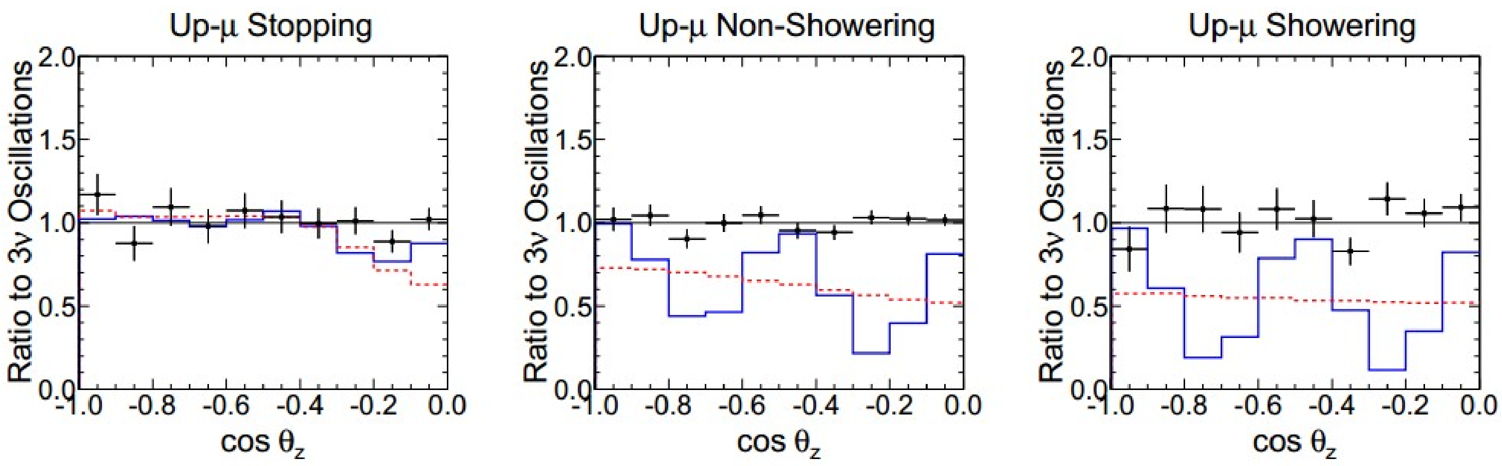

FIG. 2. (color online) Ratios of the summed SK-I through SK-IV $\cos\theta_z$ distributions relative to standard three-flavor oscillations for the UP-μ sub-samples, which are the most sensitive to the effects of LV. The stopping sub-sample (left) has a peak energy around 10 GeV, the non-showering sub-sample (center) peaks around 100 GeV, and the showering sub-sample (right) peaks around 1 TeV. The black points represent the data with statistical errors. The lines corresponds to the MC prediction including Lorentz-violating effects, with $a^{T}_{\mu\tau} = 10^{-22}$ GeV in solid blue and $c^{TT}_{\mu\tau} = 10^{-22}$ in dashed red.

Results

- No evidence of LV.
  - Limits set on the isotropic LV parameters in the eμ, μτ, and eτ sectors.
    - First limits in the μτ sector.
    - a^T limits improved by ~3 orders of magnitude
    - c^{TT} limits improved by ~7 orders of magnitude.

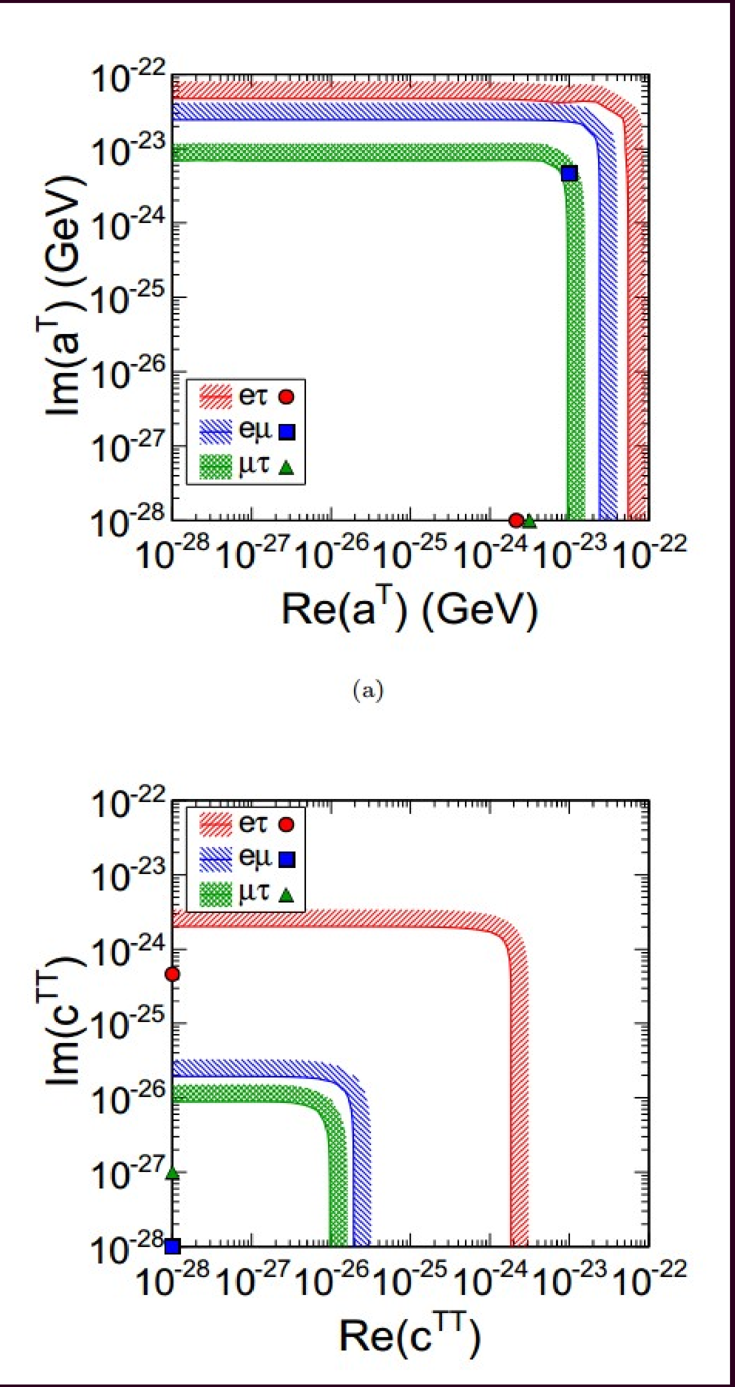

Summary

Results

- LIV violation
  - Limits set on the isotropic LV parameters in eμ, μτ, and eτ sectors.
    - First limits in the μτ sector.
    - a^T and c^{TT} limits in other sectors improved by orders of magnitude.
- NSI
  - Limits on real parts of $\varepsilon_{e\tau}$, $\varepsilon_{\mu\mu}$, $\varepsilon_{\mu\tau}$, and $\varepsilon_{\tau\tau}$.
- Sterile Neutrinos
  - Limits on $|U_{\mu 4}|^2$ and $|U_{\tau 4}|^2$
    - at MeV scale (15~100 MeV range).
    - at eV scale, limits in the 3+1 case
      - extensions to 3+N shown.

Backup

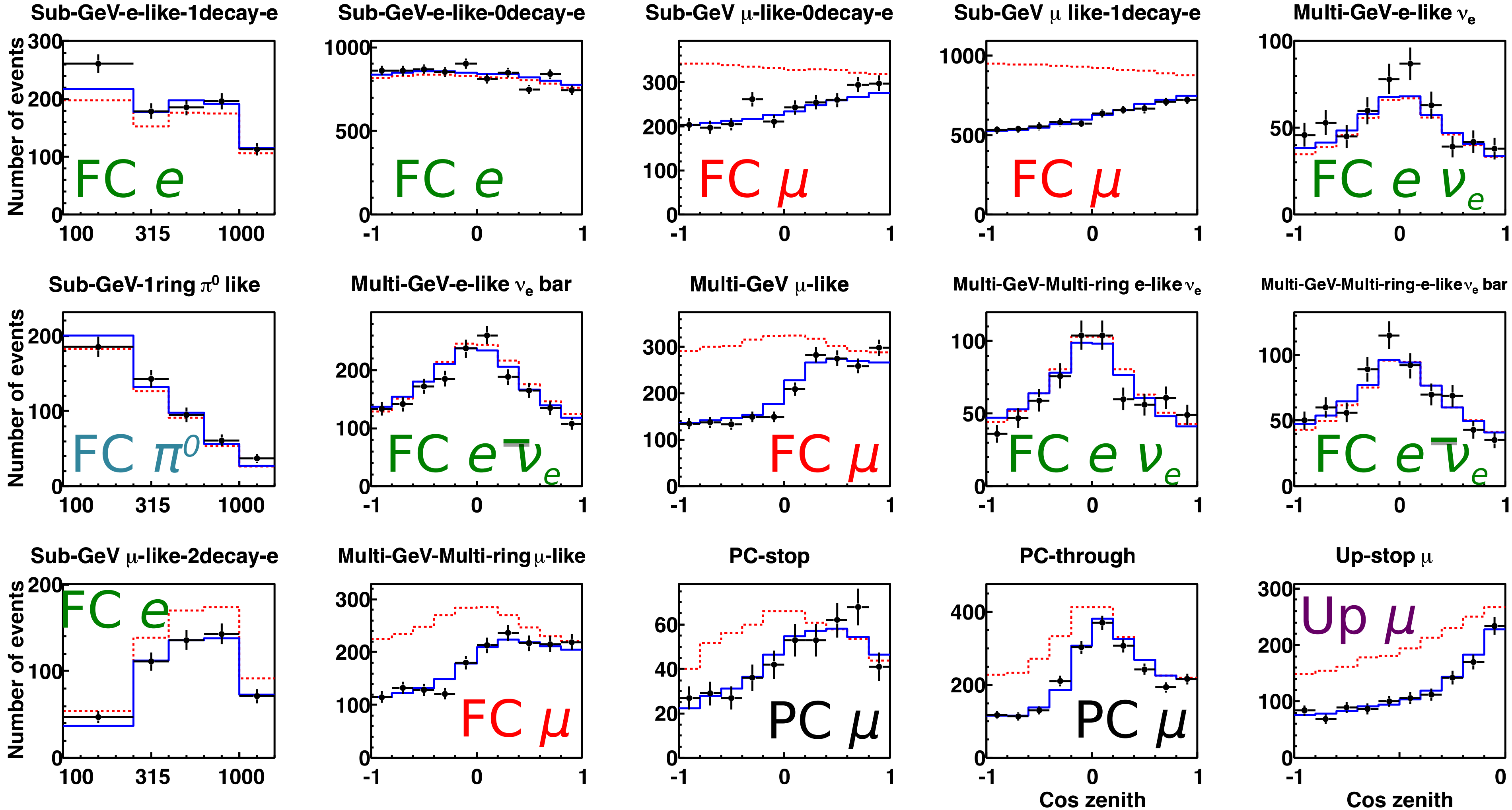

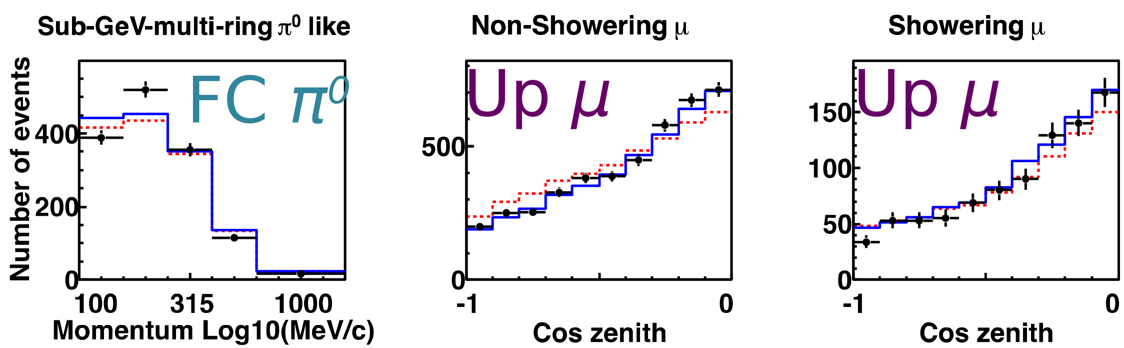

Same philosophy, more samples

Most samples binned in angle & energy

Sterile Neutrino - Basic Theory

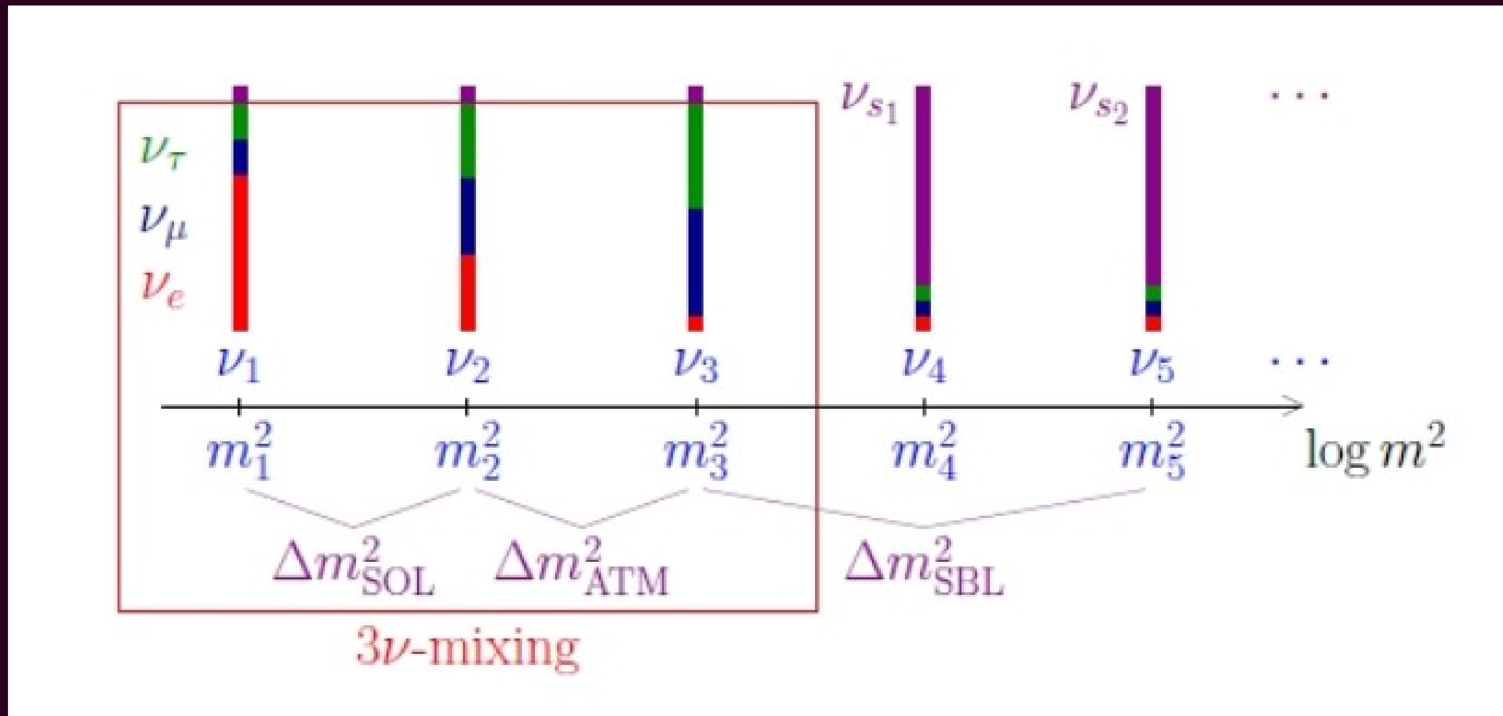

PMNS

$$U = \begin{pmatrix} U_{e1} & U_{e2} & U_{e3} & U_{e4} \\ U_{\mu 1} & U_{\mu 2} & U_{\mu 3} & U_{\mu 4} \\ U_{\tau 1} & U_{\tau 2} & U_{\tau 3} & U_{\tau 4} \\ U_{s1} & U_{s2} & U_{s3} & U_{s4} \end{pmatrix}$$

Current Limits

- Previous limits on the parameter $|U_{\mu 4}|^2$ (~2 years old)

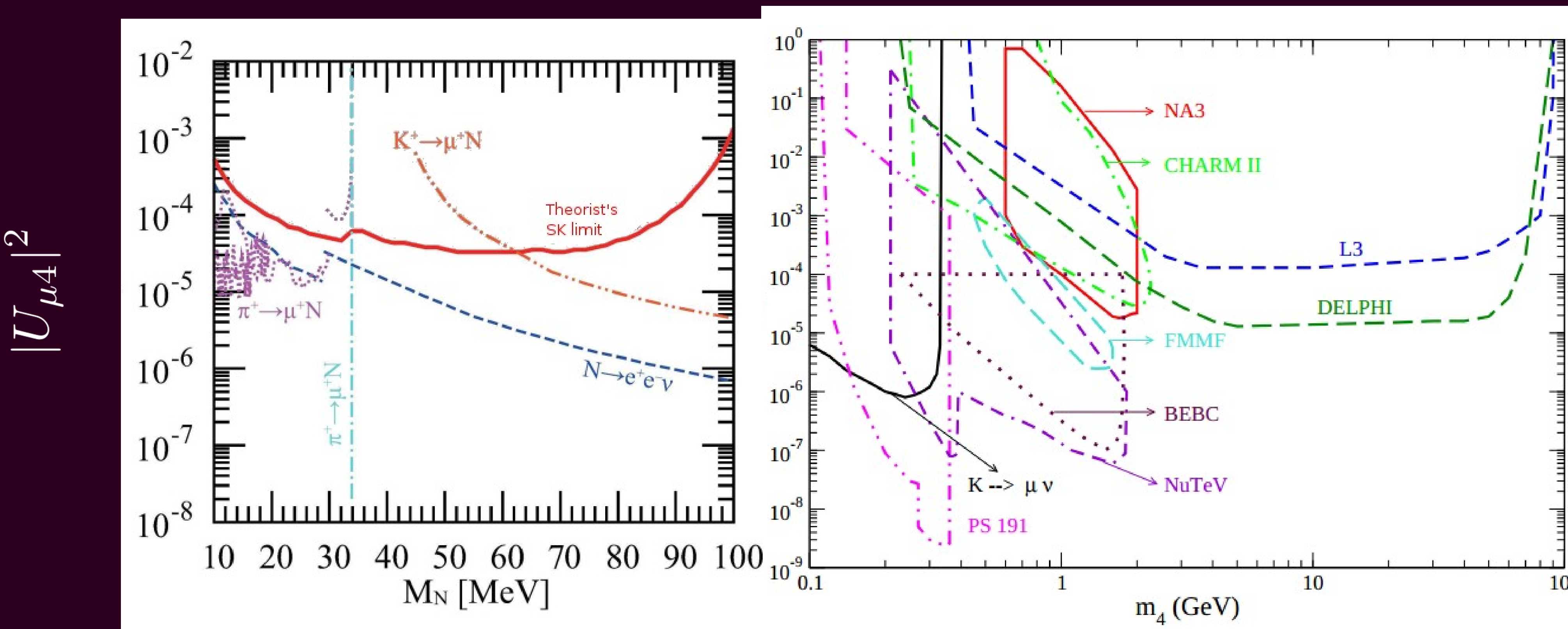

- Red line is a limit using public SK data, by T. Asaka and A. Watanabe [3] (not a Super-K collaboration paper).

Flux Simulation

- **In summary**, we will simulate the expected number of heavy-neutrino decays detected in SK, using modifications to the atmospheric neutrino flux simulation by M. Honda[4] (and detector response by Monte-Carlo).
- *Heavy neutrino creation in the atmosphere*:
  - The creation is similar to the muon (anti-)neutrino, subject to the extra mass requirements.
  - Each creation of a muon neutrino in the simulation can be reweighted, e.g. for muon decay:

$$\frac{\Gamma(\mu^- \to e^- \nu_e \nu_4)}{\Gamma(\mu^- \to e^- \nu_e \nu_\mu)} = |U_{\mu 4}|^2 (1 - 8r + 8r^3 - r^4 - 24r^2 \ln(r))$$ [3]

where

$$r = \left(\frac{m_4}{m_\mu}\right)^2$$

  - Similar reweighting for pion & kaon decays.

ν_e Appearance at 1 m/MeV?

- LSND
  - Anti-ν_e appearance in a stopped-π beam
  - L ~ 30 m, E ~ 30 MeV -> **Δm^2 ~ 1 eV^2**
- Not consistent with other oscillation measurements

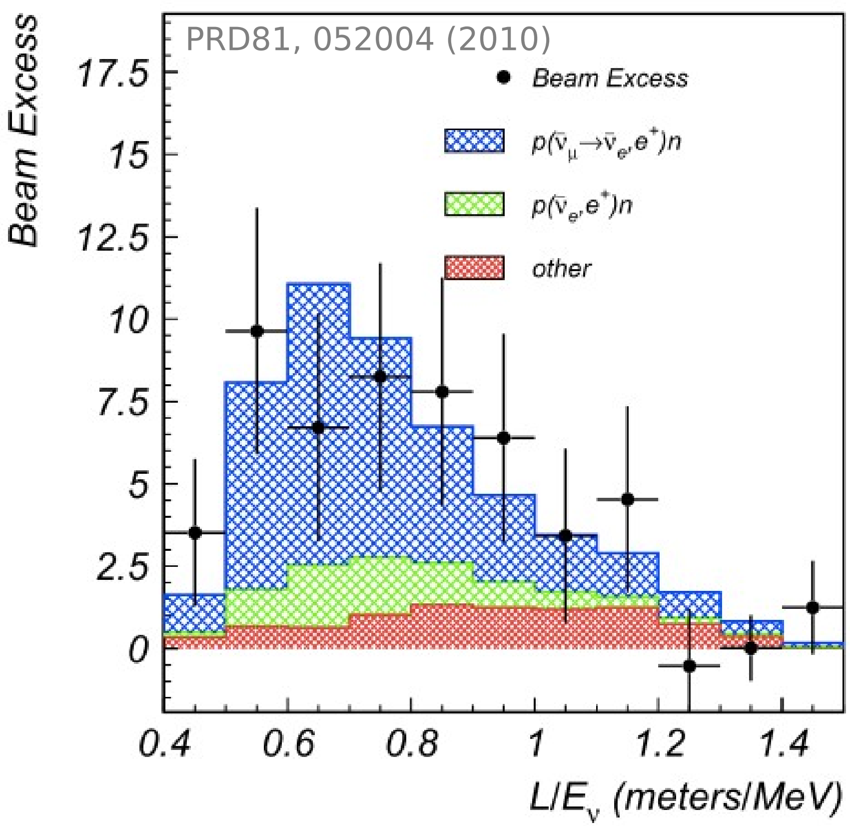

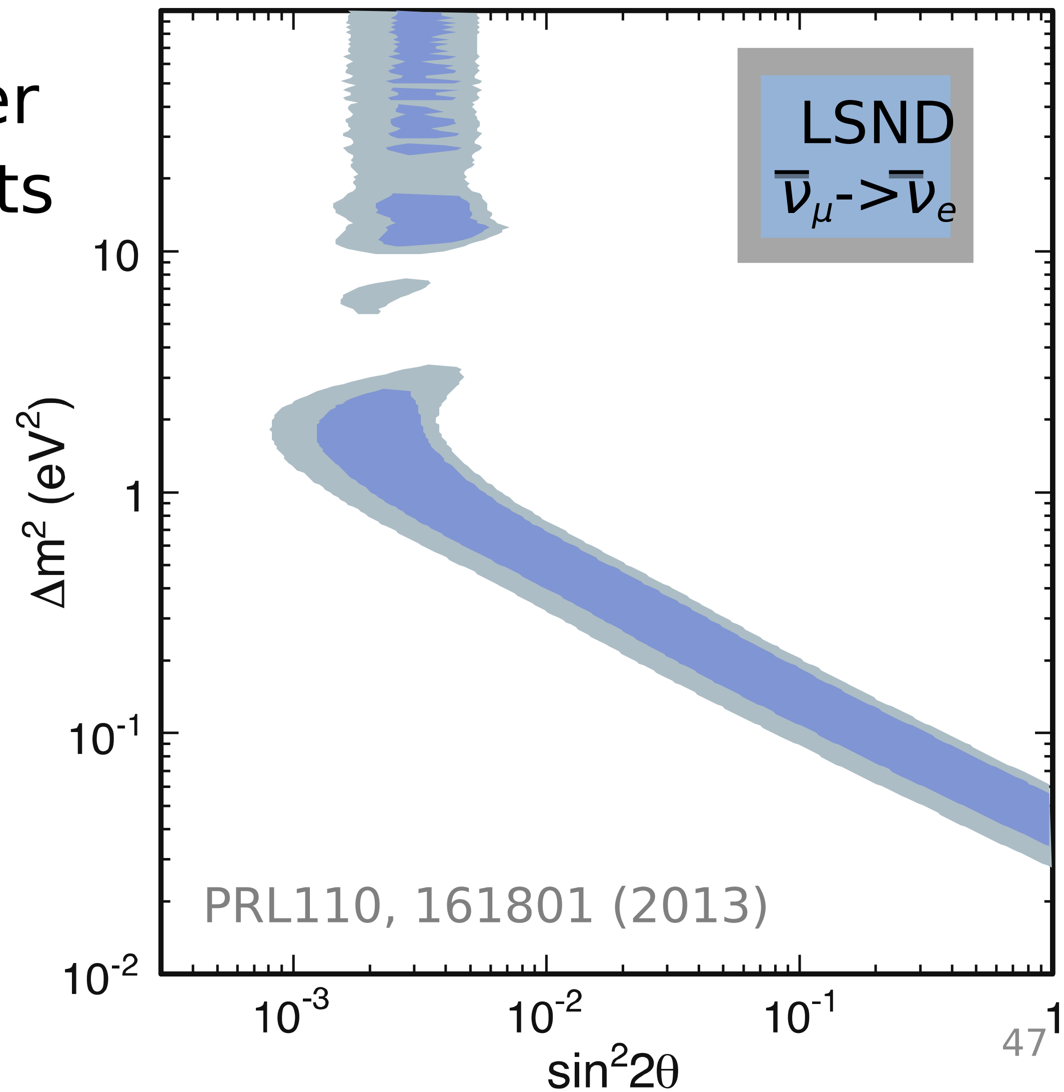

ν_e Appearance at 1 m/MeV?

- MiniBooNE
  - ν_e and anti-ν_e appearance, different beam
  - L ~ 500 m, E ~ 500 MeV
- Does not confirm LSND, but does not exclude sterile oscillations

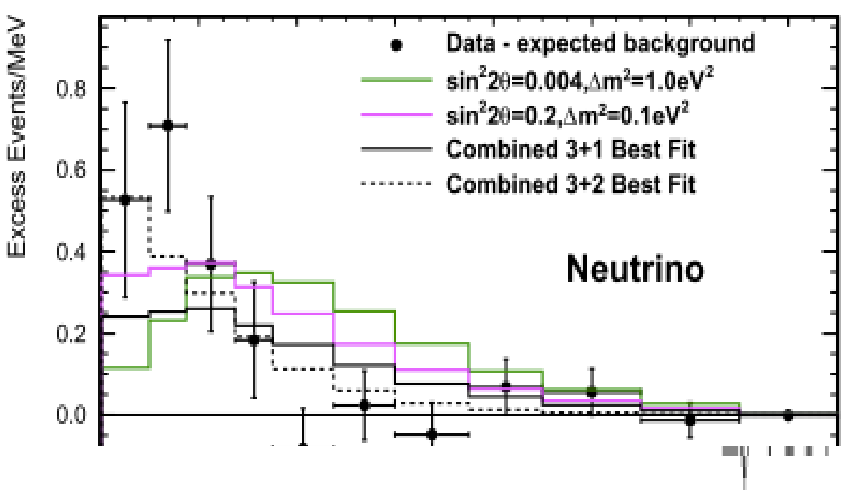

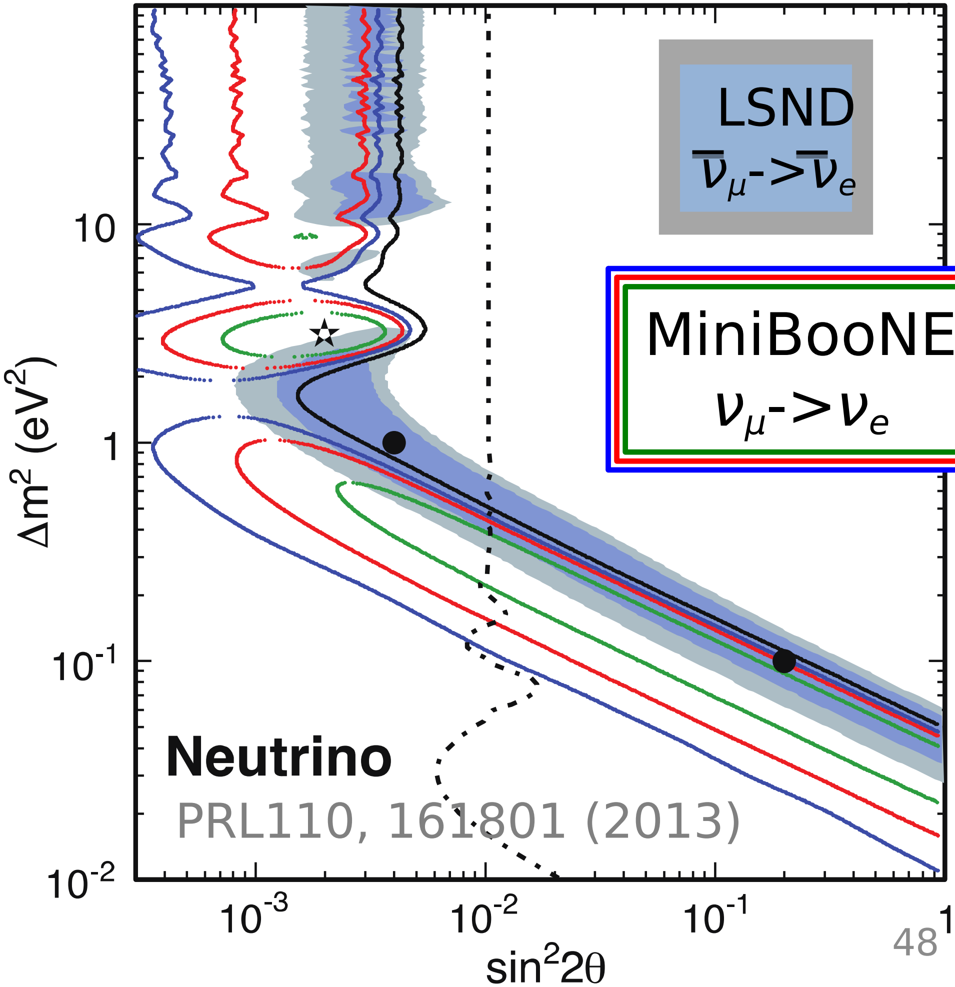

ν_e Disappearance at 1 m/MeV?

- Reactor anti-ν_e flux recalculated in 2010
- With the new flux, most short-baseline reactor experiments have deficits
  - $R_{avg} = 0.927 \pm 0.023$
  - $L \sim$ 10-100 m
  - $E \sim$ 5 MeV

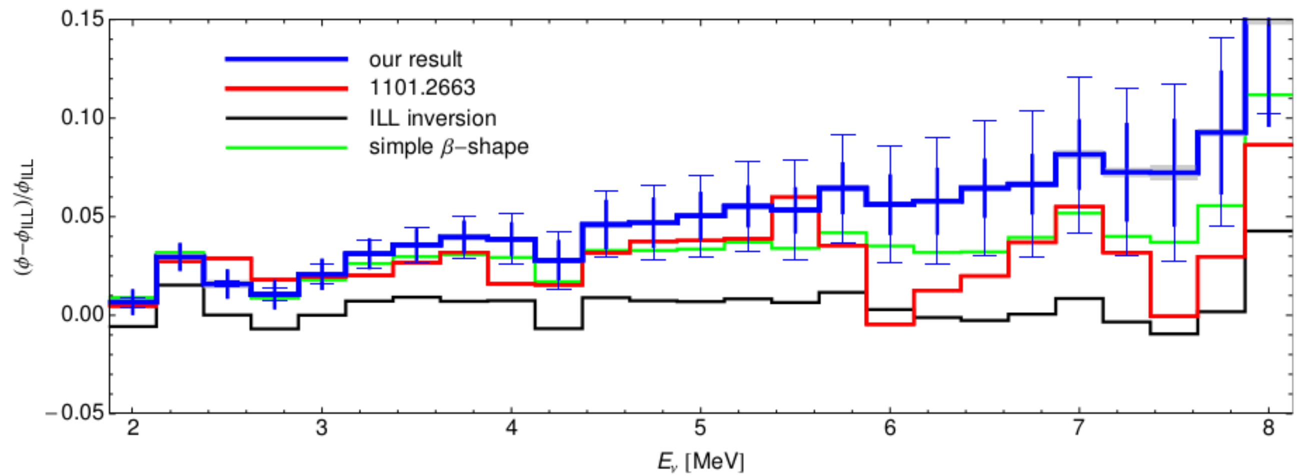

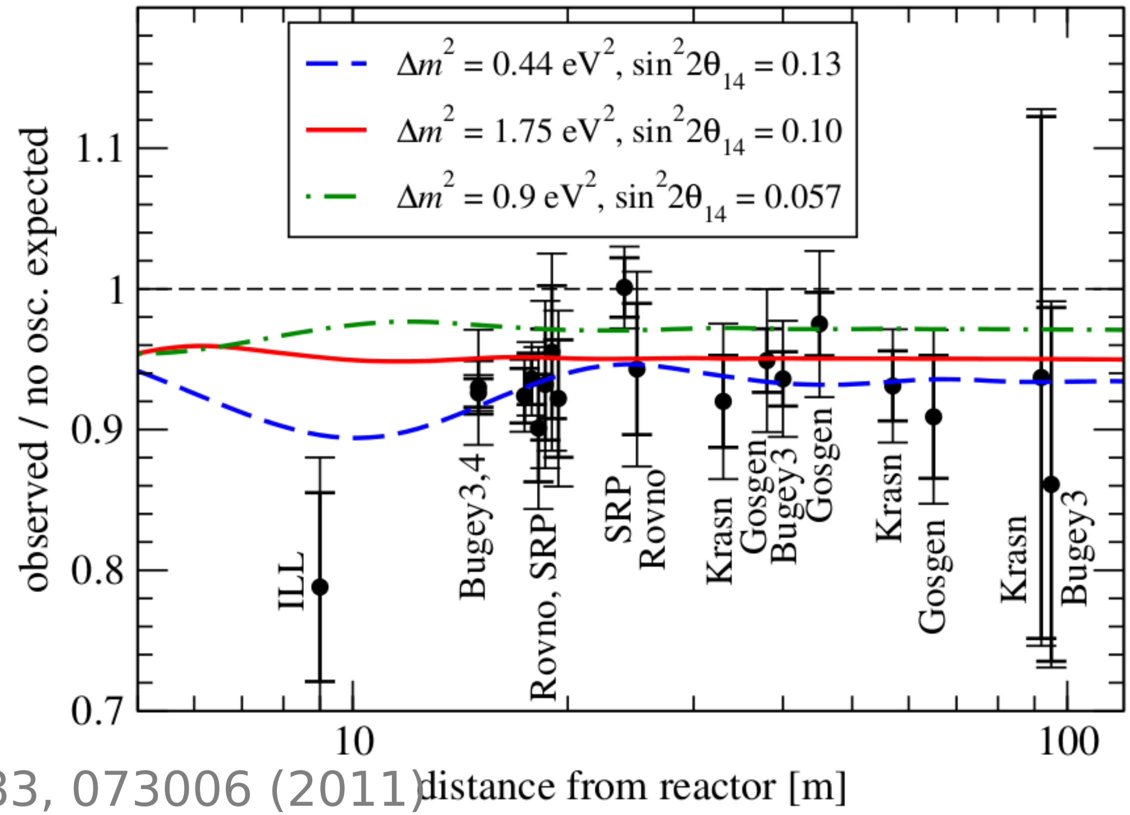

PRD83, 073006 (2011)

ν_e Disappearance at 1 m/MeV?

- Another anomaly in Gallium-based solar experiments
- Gallex and SAGE used radioactive calibration sources ^{51}Cr and ^{37}Ar
- The rates from these sources were, again, lower than expected.
  - $R_{avg} = 0.87 \pm 0.05$

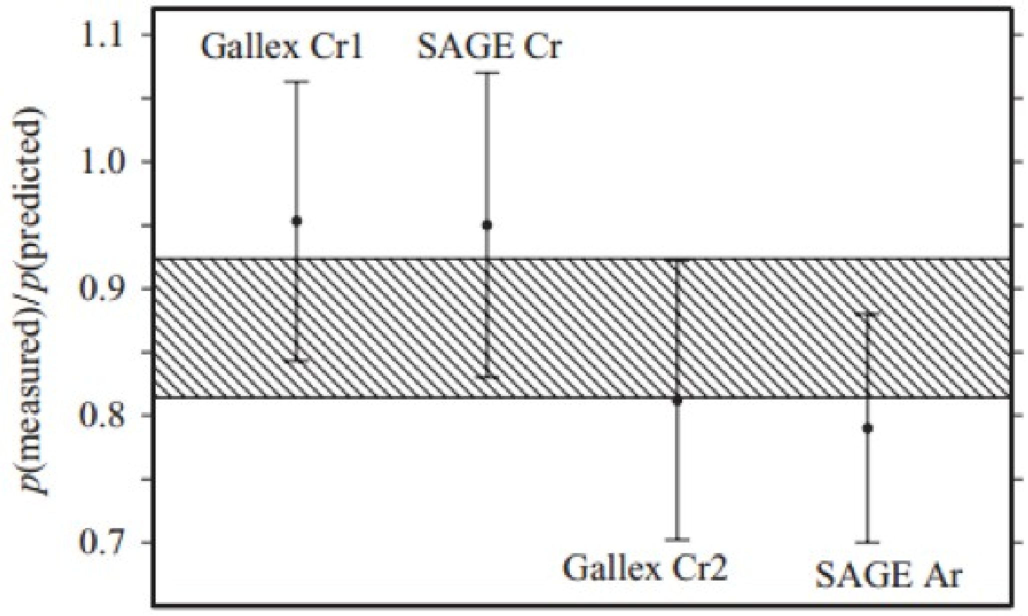

Sterile Vacuum Results

- Best fit: $|U_{\mu 4}|^2 = 0.016$
  - Shown as solid line at right
  - Dashed line shows fit without minimizing systematics
- All of the χ^2 improvement at best fit is in systematics.
  - Fit is systematically limited

Systematic	No Steriles	Best Fit
ν_μ/ν_e flux, E < 1 GeV	-0.52σ	-0.07σ
ν_μ/ν_e flux, E 1-10 GeV	-0.50σ	-0.11σ
CCQE $\boldsymbol{\nu_\mu/\nu_e}$	0.38σ	**-0.01σ**

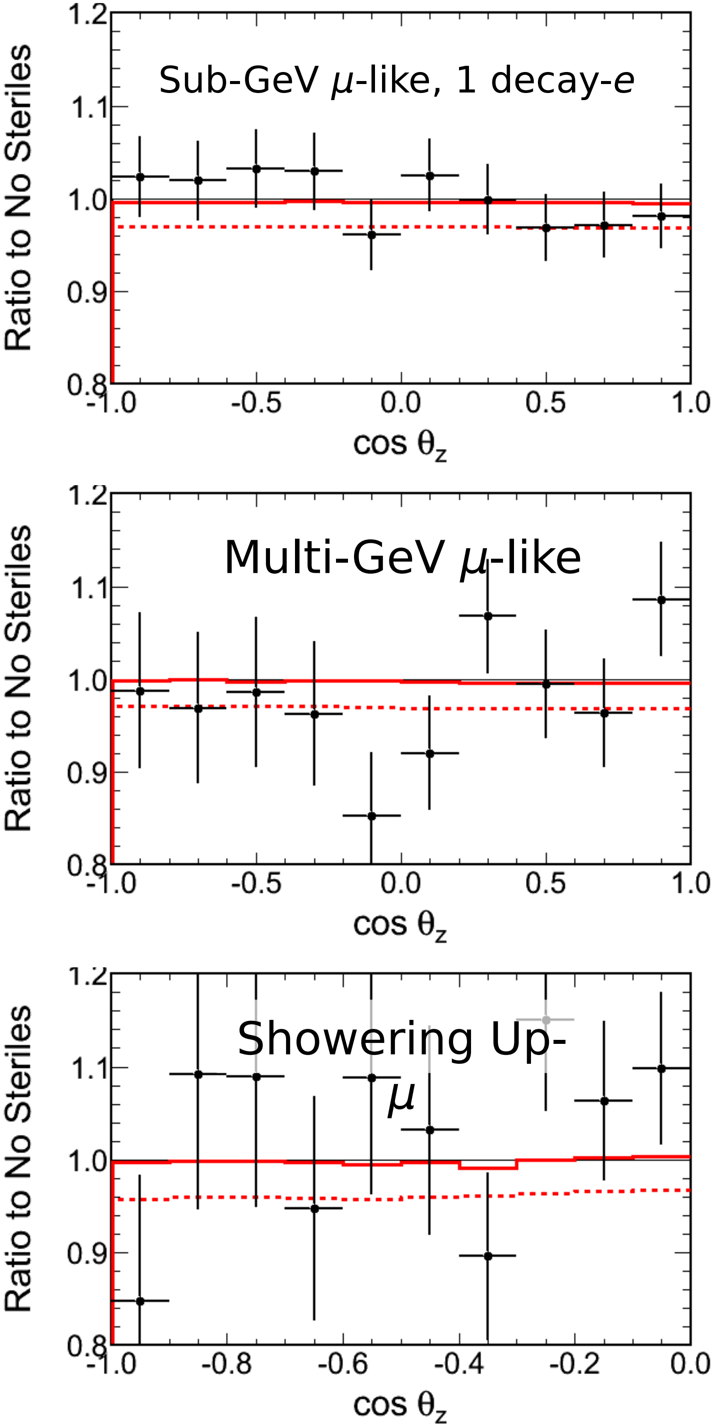

Approximations

1. No sterile-electron neutrino mixing

Following the method in Appendix C2 of [60], we can approximate the primary effect of a non-zero $|U_{e4}|^2$ by considering only its effect on the ν_e survival probability P_{ee}, taken as analogous to $P_{\mu\mu}$:

$$P_{ee} = \left(1 - |U_{e4}|^2\right)^2 P_{ee}^{(3)} + |U_{e4}|^4, \qquad \text{(B1)}$$

where $P_{ee}^{(3)}$ is the standard three-flavor ν_e survival probability. When this extra free parameter is introduced, the limit on $|U_{\mu4}|^2$ turns out to be correlated with the limit on $|U_{e4}|^2$, as shown in the sensitivity contours in

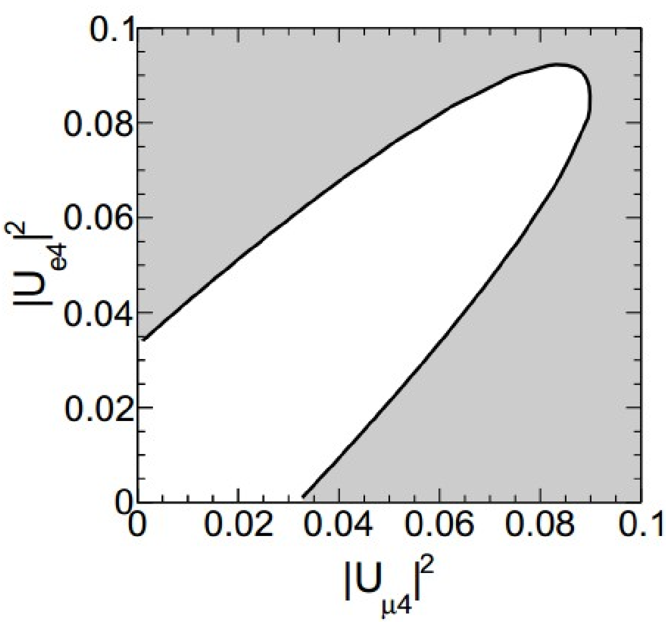

FIG. 9. The 90% sensitivity contour for the sterile vacuum fit with the effect P_{ee} from Eq. (B1) included. Allowing the freedom in the electron sample normalization reduces the sensitivity to $|U_{\mu4}|^2$ as can be seen from the bowing outward on the right side of the contour. Note that on this plot $|U_{\mu4}|^2$ is shown in linear scale so the correlation with $|U_{e4}|^2$ is clear.

Fig. 9. With $|U_{e4}|^2$ unconstrained, the 90% MC sensitivity to $|U_{\mu4}|^2$ becomes 0.067, significantly weaker than the 0.024 sensitivity with the assumption of $|U_{e4}|^2 = 0$. However, when the Bugey constraint is included by adding the penalty term

$$\chi^2_{\text{penalty}} = \left(|U_{e4}|^2/0.012\right)^2, \qquad \text{(B2)}$$

again following the technique of [60], the sensitivity becomes 0.029, very close to the original sensitivity.

2. No three-flavor matter effects in the no-ν_e fit

The main effect of setting θ_{13} to zero in the no-ν_e fit, eliminating Multi-GeV ν_e appearance, was already discussed in Eq. (5.3). However, this assumption has a second effect: it eliminates the distortion in the ν_μ survival probability from matter effects in the Earth. These distortion can be seen in the few-GeV region for the most upward going events ($\cos\theta_z \approxeq -1$) in Fig. 2(a).

Neglecting this matter effect turns out to have little effect on the $|U_{\tau4}|^2$ limit. A sensitivity fit using the no-ν_e model to a MC prediction made using the full three-flavor oscillation probability which includes these distortions finds a best fit at $|U_{\tau4}|^2 = 0$ and $|U_{\mu4}|^2$ equal to its minimum value (it is binned in log scale and so does not go to zero). The three flavor distortions in the ν_μ survival probability turn out to be relatively small (at most a few percent in the PC through-going and stopping UP-μ samples) and to not affect the through-going UP-μ samples which are distorted significantly by the sterile matter effects.

Approximations

3. Sterile-induced fast oscillations

This assumption posits that the oscillations driven by Δm^2 are so fast that individual oscillation periods cannot be resolved in the experiment and that functions of Δm^2 can be replaced with their average values:

$$\sin\left(\frac{\Delta m^2 L}{4E}\right) \to \langle \sin \rangle = 0 \tag{B3}$$

$$\sin^2\left(\frac{\Delta m^2 L}{4E}\right) \to \langle \sin^2 \rangle = \frac{1}{2}. \tag{B4}$$

However, since the phase in these terms depends on L and E as well as Δm^2, the ranges over which they are valid could vary for the different samples used in the analysis. For a sufficiently small Δm^2, this fast oscillation assumption will break down, and the higher the energy and shorter the path length, the larger of a value of Δm^2 that is invalid. We can estimate this lower limit by calculating the value of $\sin^2(\Delta m^2 L/4E)$ for many MC events in the various SK samples (FC Sub- and Multi-GeV, PC, and UP-μ) at a range of possible values of Δm^2. The average is then calculated from the event-by-event values at each Δm^2 and the point where the actual average deviates significantly from one half can be found. These averages vs. Δm^2 for the four samples can be seen in Fig. 10.

Setting a threshold of 5% error on the value of $\sin^2$, we find that the fast oscillation sample is valid until approximately 10^{-1} in all four samples. The highest limit is 0.13 in the PC sample where there are both high energies and the very short track lengths from down-going events.

Meeting this assumption only sets the bottom of the valid Δm^2 range. The upper limit on the mass for which the limits are valid is set by the requirement that the mass-splitting is sufficiently small that the neutrinos remain coherent. A sufficiently heavy neutrino, approximately 1 keV or so, will separate from the other light neutrinos and thus not be able to participate in oscillations.

“Heavy” Sterile Neutrinos

- A state $m_4 \gtrsim \mathrm{keV}$ is separated from the oscillation effects.
- The phenomenology varies depending on the mass, and in some cases we may have observable decay products.
  - For example, take $m_4 \sim MeV$
    - Motivated by e.g. νMSM - standard Seesaw mechanism, but Majorana masses M_I are chosen below electroweak scale.

$$\mathcal{L} = \mathcal{L}_{SM} + i\bar{\nu}_{s_I}\partial_\mu\gamma^\mu\nu_{s_I} - \left(F_{\alpha I}\,\bar{L}_\alpha\nu_{s_I}\tilde{\phi} - \frac{M_I}{2}\,\bar{\nu}^c_{s_I}\nu_{s_I} + h.c.\right)$$

with left-handed leptons L_α, Yukawa couplings $F_{\alpha I}$, and Higgs ϕ.

Flux Simulation

- *Decay of the heavy neutrino*:
  - Approximately 12% of the decays are in the visible mode.

$$\Gamma(\nu_4 \to 3\nu) = \frac{G_F^2 m_4^5 |U_{\mu 4}|^2}{192\pi^3}$$

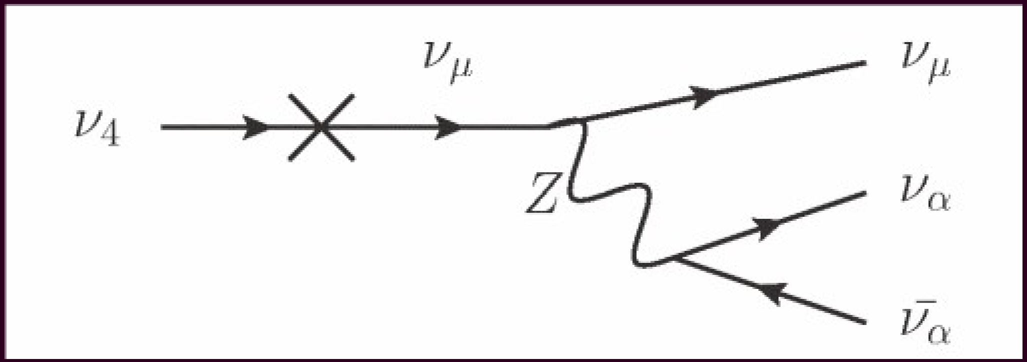

$$\Gamma(\nu_4 \to e^+ e^- \nu) = \Gamma(\nu_4 \to 3\nu)(\frac{1}{4} - \sin^2\theta_W + 2\sin^4\theta_W)$$

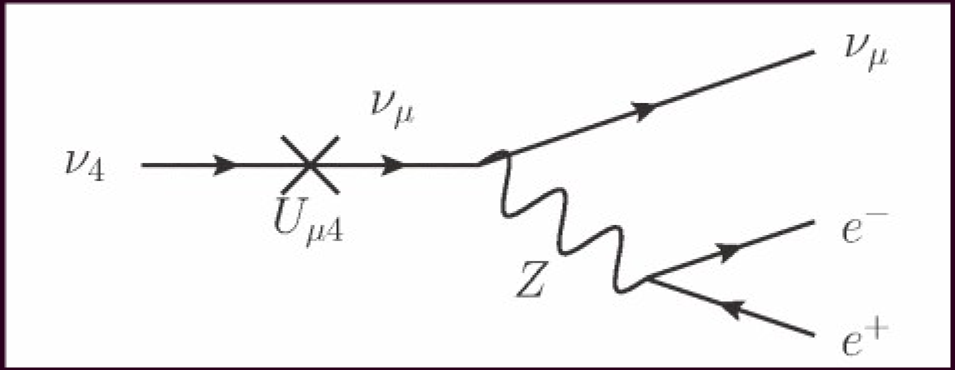

Flux Simulation

- Thus, we can estimate the probability of a heavy-neutrino to decay to the visible mode inside of SK, depending on the mass, travel distance to SK, and $|U_{\mu 4}|^2$.
  - For this plot, we set
    .
  - It can be seen that there will be a dependence on travel length that gets stronger with increasing mass.
    - In SK, this means a zenith angle dependence of the signal.
  - A similar dependence is seen for $|U_{\mu 4}|^2$ for a fixed mass.

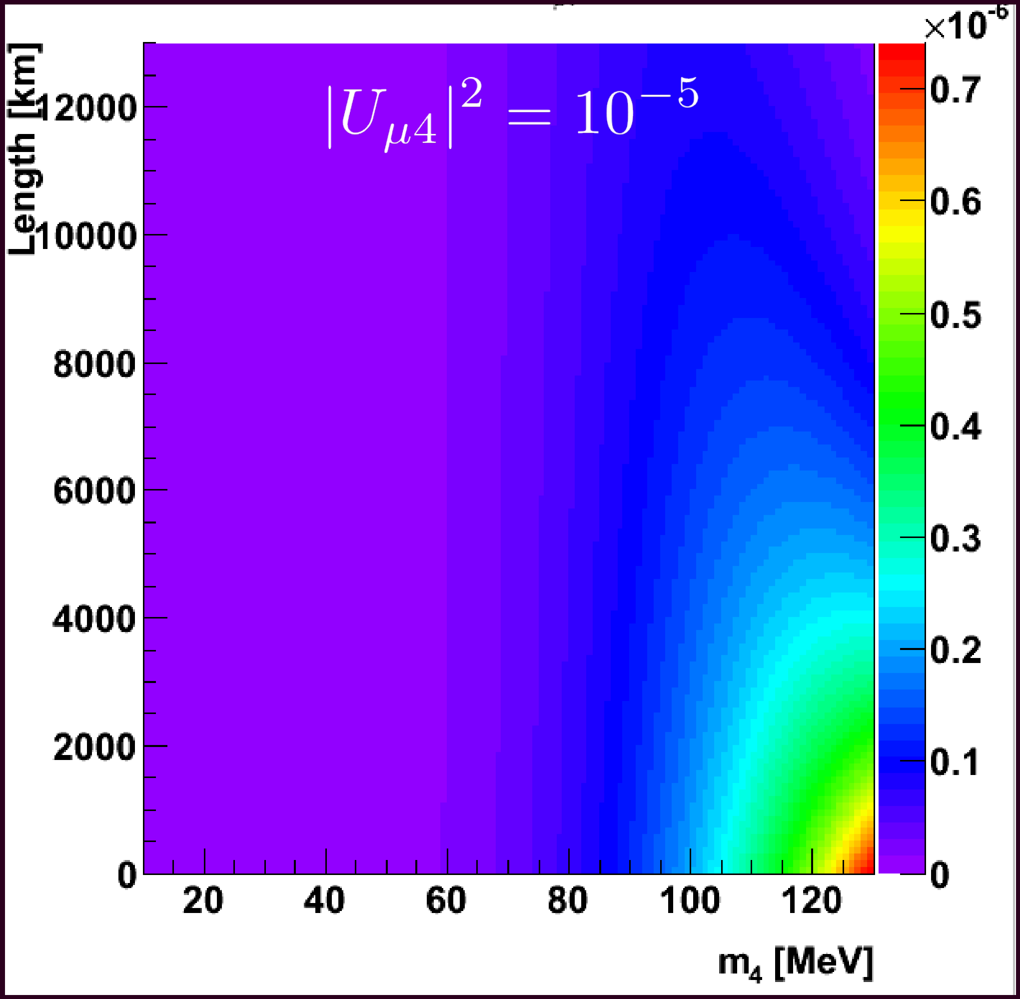

2D distributions

- Events are binned in 2d.
  - Not actually the final binning (can't find those plots...)

Background (atmospheric MC)

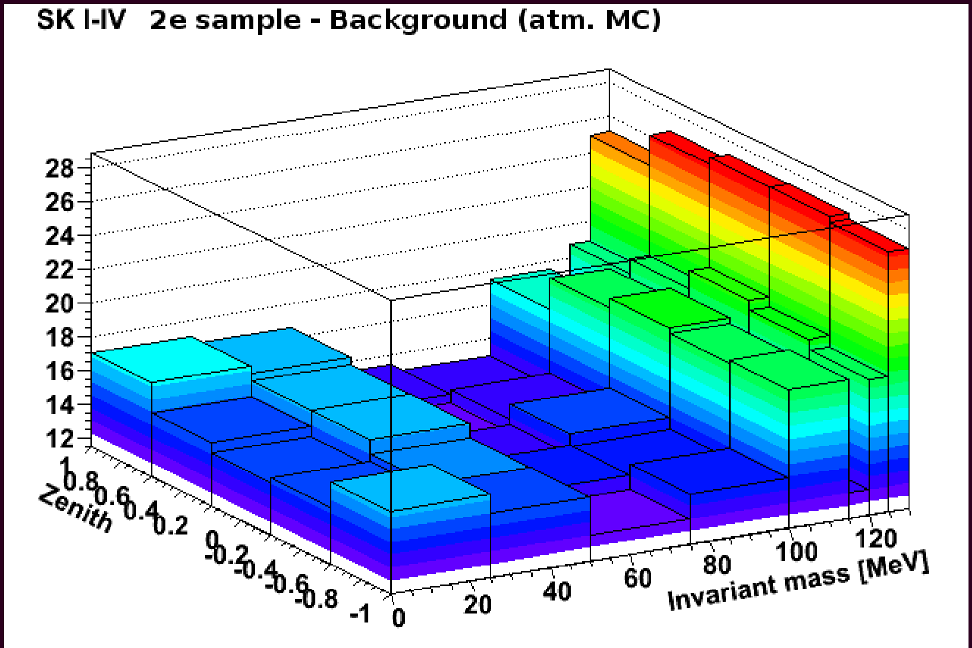

Signal (sterile decay)

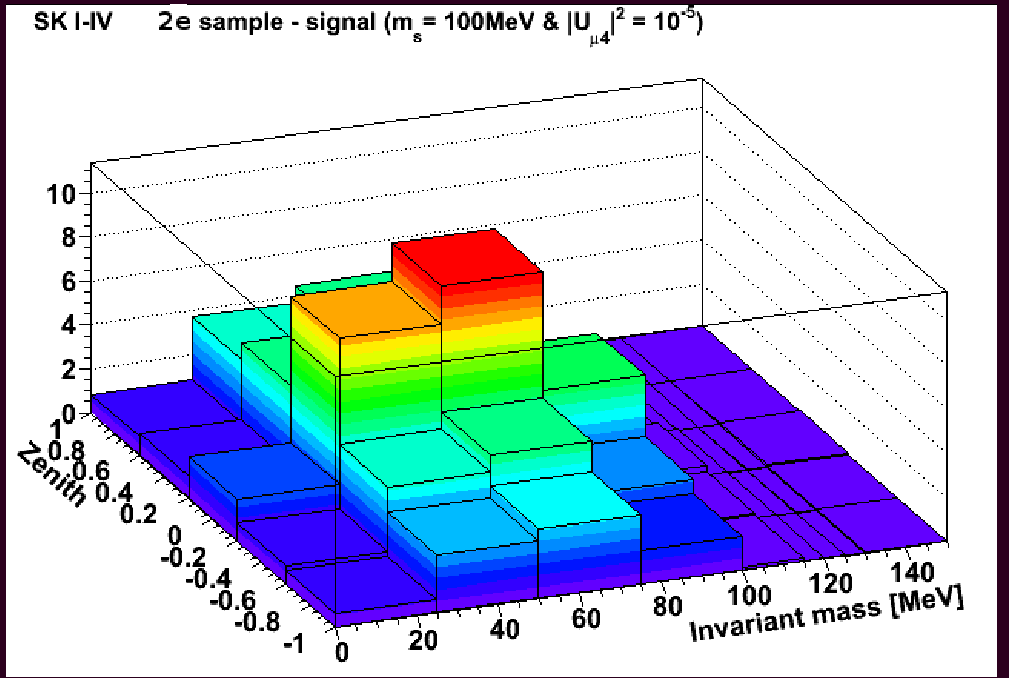

Fitting Procedure

- A fit is performed for $|U_{\mu 4}|^2$ separately at each mass point.
  - The binning of the zenith & invariant mass distributions was optimized using the Monte-Carlo.
  - For this study, 44 (*21*) systematic errors from the SK MC are applicable to the atmospheric background MC (*sterile MC*).
- The fit is a χ^2-minimization, with systematic errors included in the fit using the method of penalty terms ("error pulls").

$$\chi^2 = 2\sum_{i=1}^{\text{nbins}} \left(z_i - N_i^{\text{obs}} + N_i^{\text{obs}} \ln \frac{N_i^{\text{obs}}}{z_i} \right) + \sum_{j=1}^{N_{\text{syserr}}} \left(\frac{\epsilon_j}{\sigma_j}\right)^2$$

$$z_i = \alpha \cdot N_i^{\text{back}} \left(1 + \sum_{j=1}^{N_{\text{syserr}}} f_i^j \frac{\epsilon_j}{\sigma_j}\right) + \beta \cdot N_i^{\text{sig}} \left(1 + \sum_{j=1}^{N_{\text{syserr}}} f_i^j \frac{\epsilon_j}{\sigma_j}\right)$$

$N_i^{obs}, N_i^{sig}, N_i^{back}$ are the data, signal MC, background MC

ϵ_j are the pull terms for each error

f_i^j are the fractional changes by a $\sigma_j = 1$ pull

α is background MC normalization, and β is related to $|U_{\mu 4}|^2$

Detection Efficiency

- Some event displays at 30 MeV

→ detection efficiency is ~25%,
but mis-reconstruction rate
is also a little high.

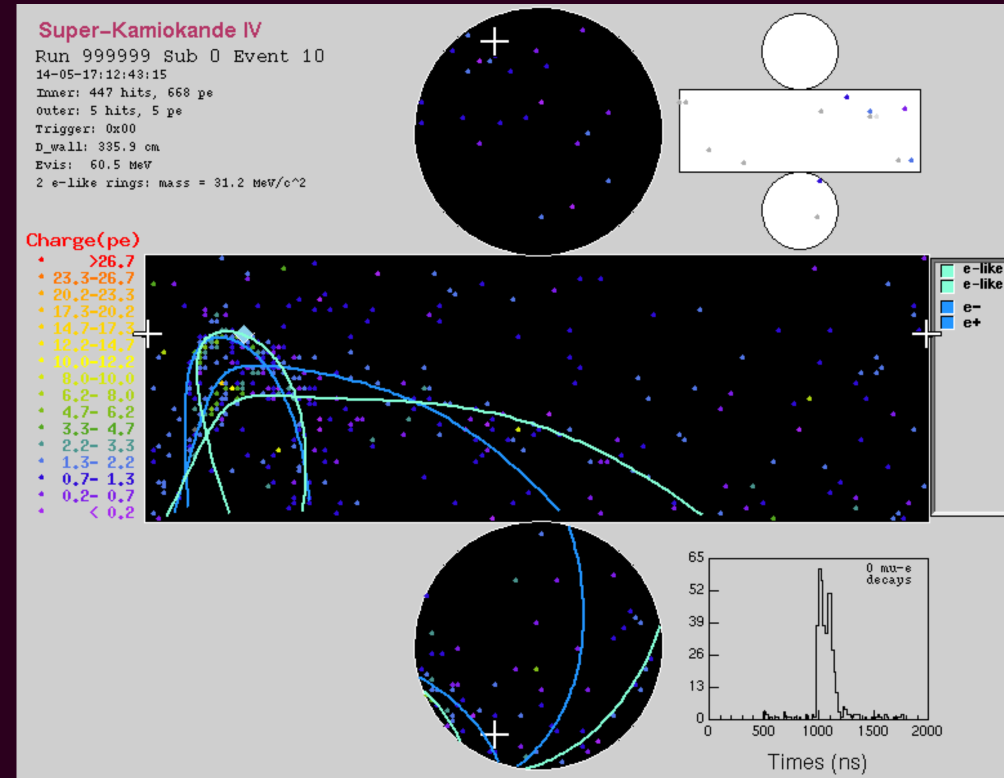

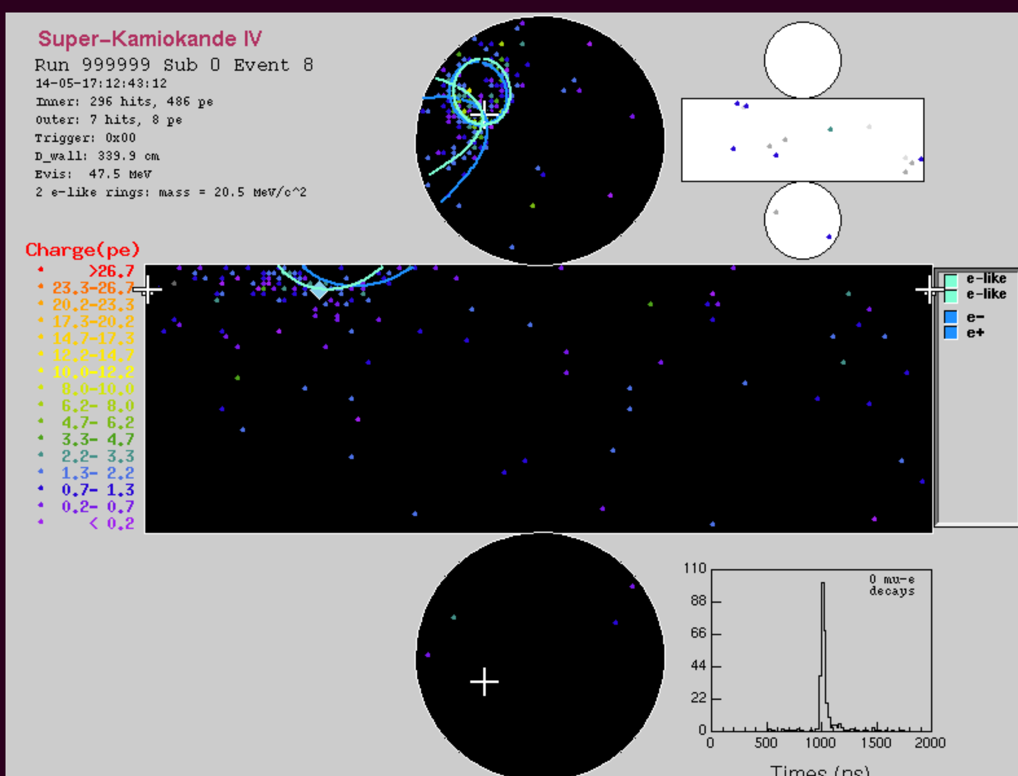

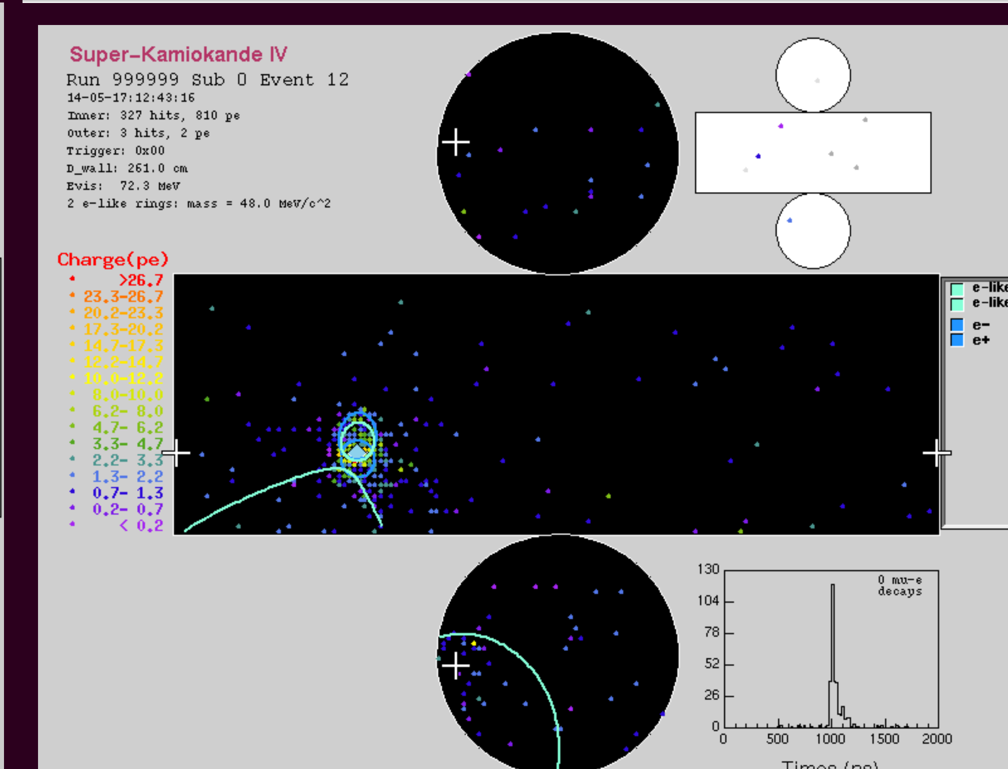

Final Fit to Data

• An example fit at sterile mass = 50 MeV, shown by *final analysis bins*
→ Data / MC comparison at best-fit point, and 90%-confidence exclusion point

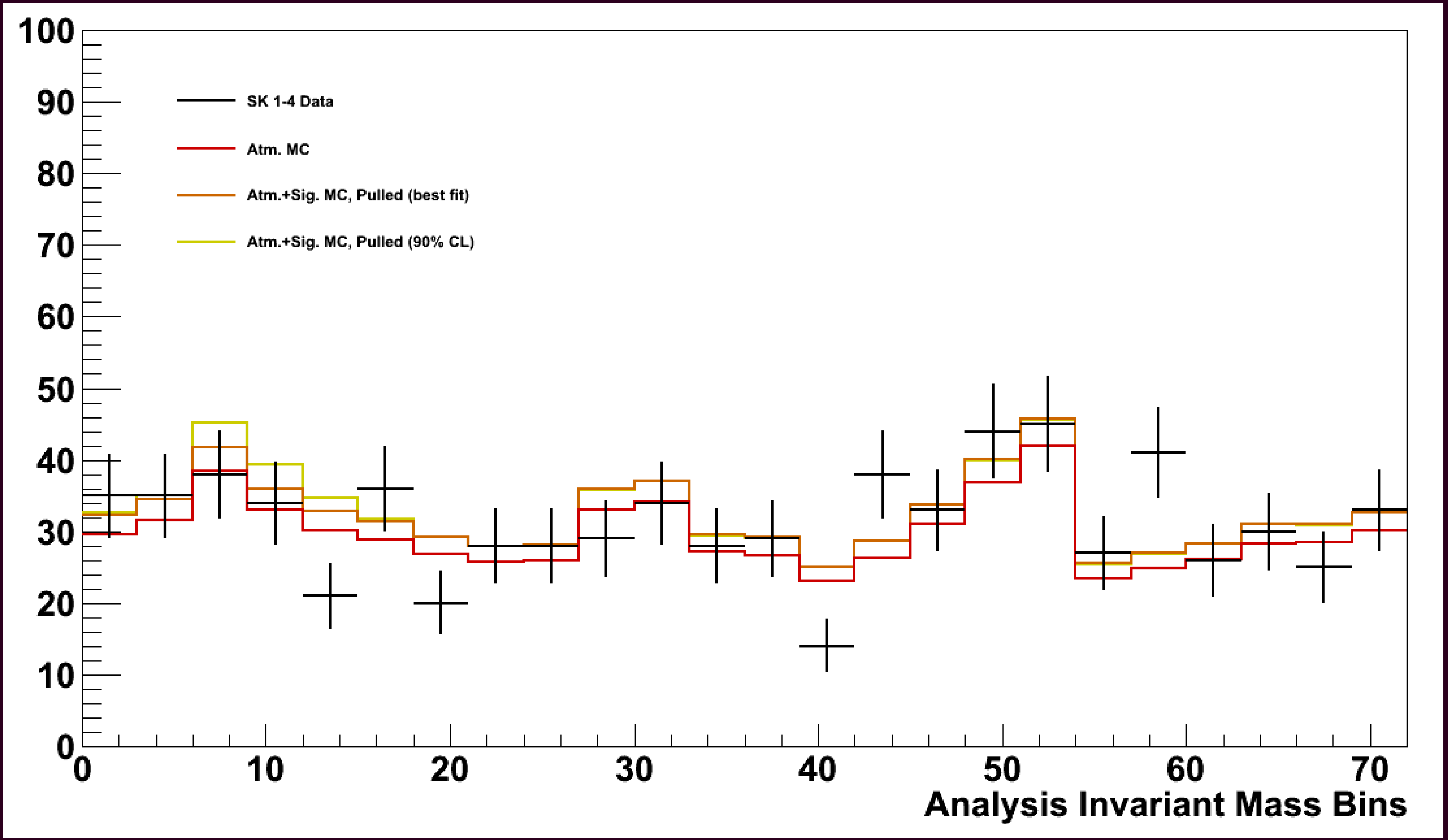

Justification for Simplified Matrix Element

- From previous limits, electron-mixing is ruled out at 2-3 orders of magnitude below muon- mixing (thanks to double-beta decay experiments), so seems negligible.

- Atmospheric decays (from Pion, Kaon, Muon) involve the charged current, so Tau mixing cannot be involved (in this energy range).

- Sterile decay can involve a Tau, with the same channels as Muon, so the final results can be interpreted instead as a limit on sqrt $|U_{\mu 4}|^2 \left(|U_{\mu 4}|^2 + |U_{\tau 4}|^2\right)$

More Phenomenology

- Pion decay rates

$$\frac{\Gamma(\pi^- \to \mu^- \nu_4)}{\Gamma(\pi^- \to \mu^- \nu_\mu)} = |U_{\mu 4}|^2 \sqrt{1 - 2(r_4 + r_\mu) + (r_4 - r_\mu)^2}\, \frac{r_4 + r_\mu - (r_4 - r_\mu)^2}{r_\mu (1 - r_\mu)^2}$$

$$r_4 = \left(\frac{m_4}{m_\pi}\right)^2$$

$$r_\mu = \left(\frac{m_\mu}{m_\pi}\right)^2$$

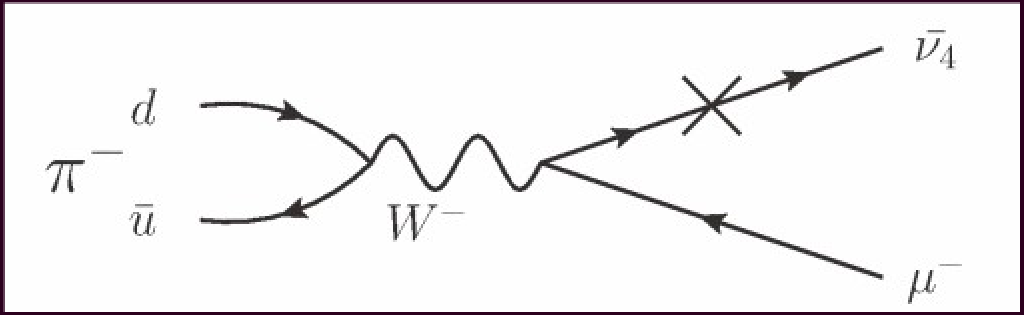

- Kaon decay:
  $K^\pm \to$ mostly 2-body decays (as the pion decay)
  $K^0 \to$ 3-body decay
  Just using an approximation
  for this one...

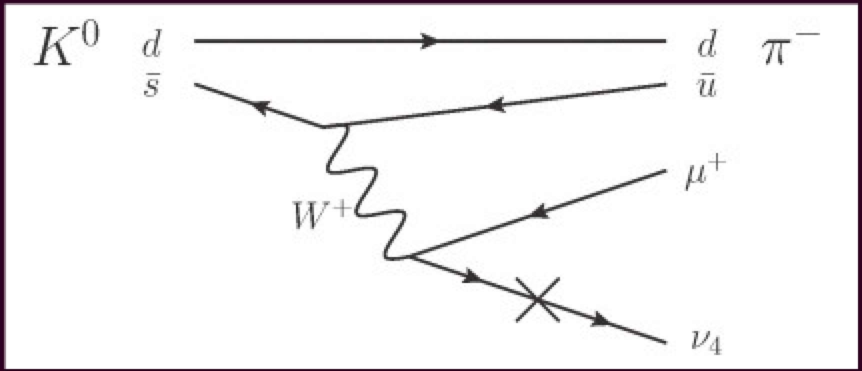

More Phenomenology

- Extension to higher sterile masses fairly simple using just W / Z branching ratios
  → would have to consider more decay samples in the analysis

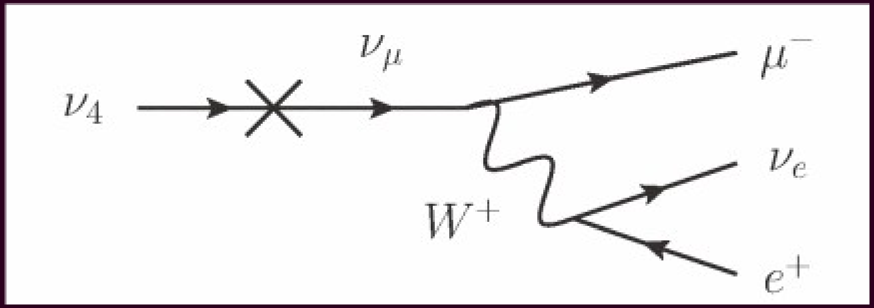

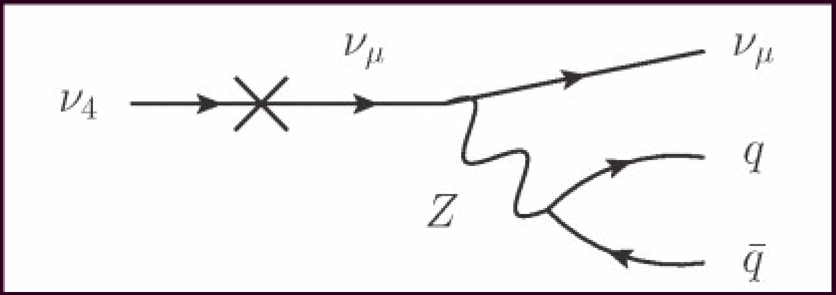

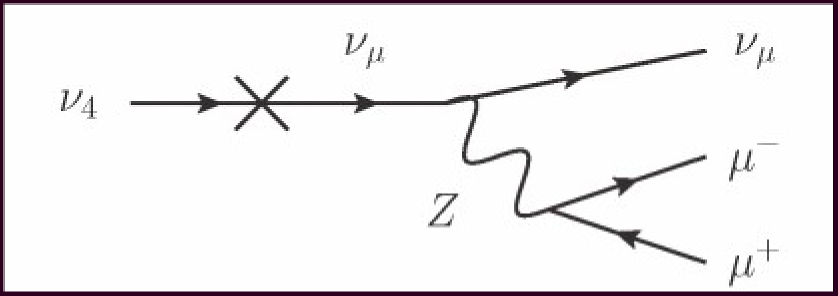

Other Possible Variables

- Use inner angle as a separation variable
  - Need to use e.g. Poisson likelihood due to low events per bin.

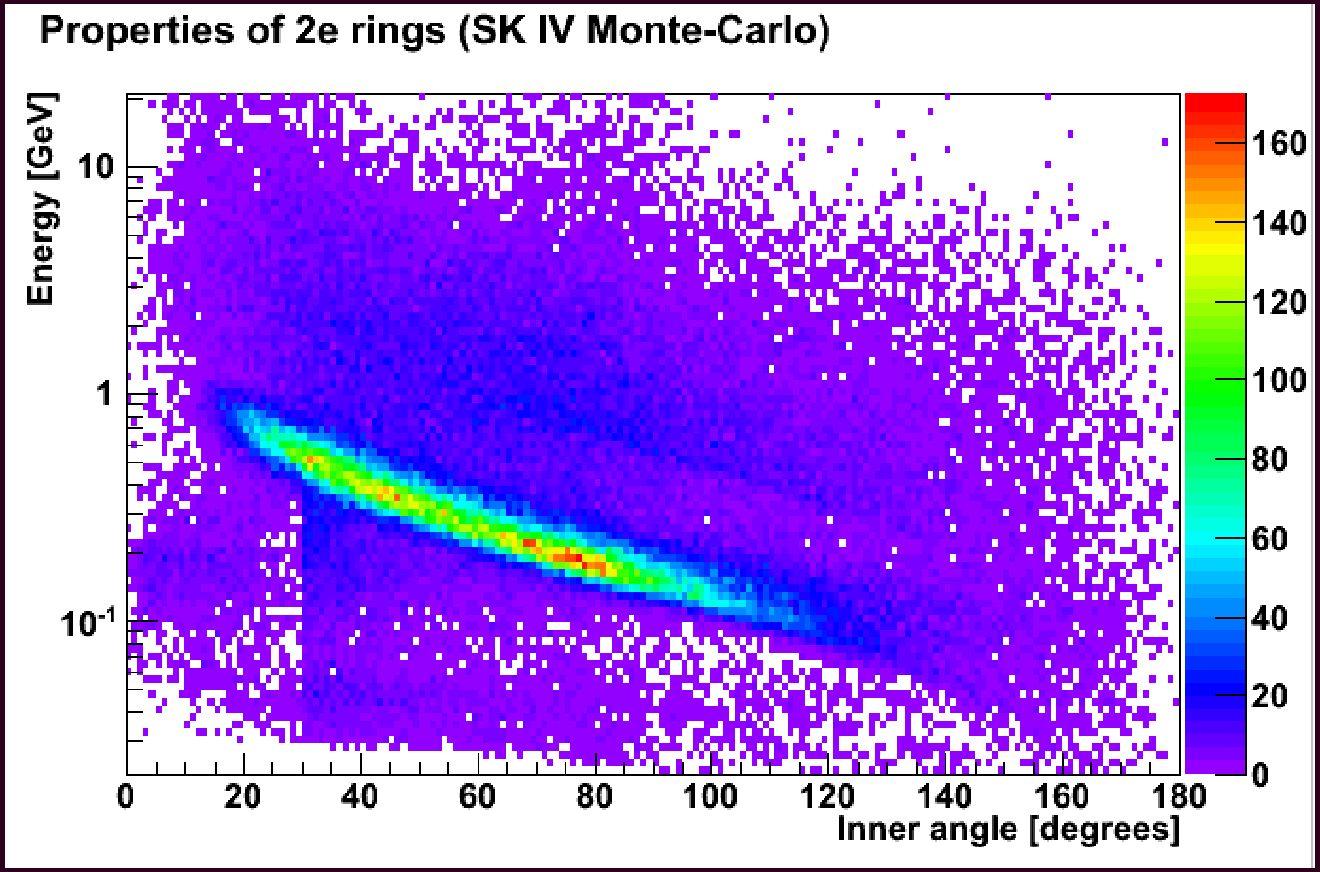

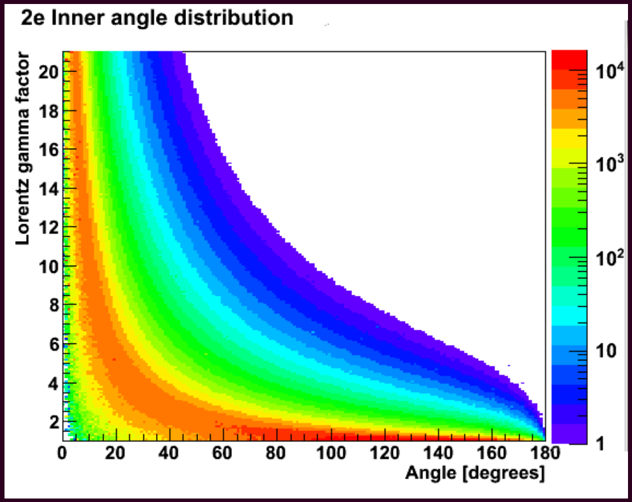

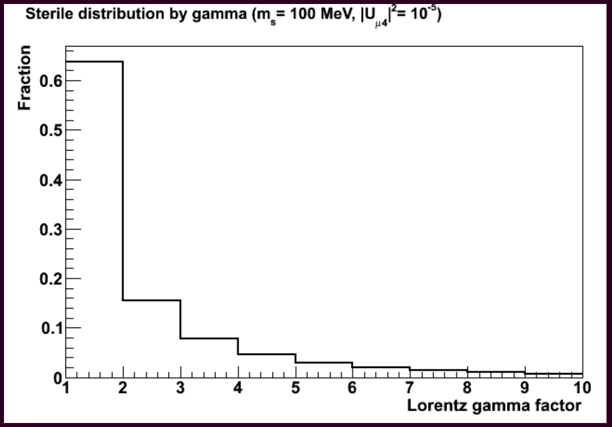

References

References for the sterile - decay study

[1] T. Asaka and M. Shaposhnikov, Phys. Lett. B620 17-26 (2005)

[2] C. F. Wong, Durham University PhD Thesis 4931

[3] T. Asaka and A. Watanabe, arXiv:1202.0725 [hep-ph]

[4] M. Honda, Phys. Rev. D83 123001 (2011)

[5] G. Bernardi et al., Phys. Lett. B166 479 (1986)

Two-flavour approach

- Survival probability is somewhat complicated

$$P_{\nu_\mu \to \nu_\mu} = 1 - P_{\nu_\mu \to \nu_\tau} = 1 - \sin^2 2\Theta \sin^2 \left(\frac{\Delta m_{23}^2 L}{4E} R \right) . \tag{2}$$

The effective mixing angle, Θ, and the correction factor to the oscillation wavelength, R, are given by

$$\begin{aligned}
\sin^2 2\Theta &= \frac{1}{R^2} \left(\sin^2 2\theta + R_0^2 \sin^2 2\xi + 2R_0 \sin 2\theta \sin 2\xi \right) , \\
R &= \sqrt{1 + R_0^2 + 2R_0 (\cos 2\theta \cos 2\xi + \sin 2\theta \sin 2\xi)}, \\
R_0 &= \sqrt{2} G_F N_f \frac{4E}{\Delta m^2} \sqrt{|\varepsilon|^2 + \frac{\varepsilon'^2}{4}}, \\
\xi &= \frac{1}{2} \tan^{-1} \left(\frac{2\varepsilon}{\varepsilon'} \right) ,
\end{aligned} \tag{3}$$

Calculation of LV Oscillation Probabilities

Hamiltonian:

$$H = U \begin{pmatrix} 0 & 0 & 0 \\ 0 & \frac{\Delta m_{21}^2}{2E} & 0 \\ 0 & 0 & \frac{\Delta m_{31}^2}{2E} \end{pmatrix} U^\dagger \pm \sqrt{2} G_F \begin{pmatrix} N_e & 0 & 0 \\ 0 & 0 & 0 \\ 0 & 0 & 0 \end{pmatrix} \pm \begin{pmatrix} 0 & a_{e\mu}^T & a_{e\tau}^T \\ (a_{e\mu}^T)^* & 0 & a_{\mu\tau}^T \\ (a_{e\tau}^T)^* & (a_{\mu\tau}^T)^* & 0 \end{pmatrix} - E \begin{pmatrix} 0 & c_{e\mu}^{TT} & c_{e\tau}^{TT} \\ (c_{e\mu}^{TT})^* & 0 & c_{\mu\tau}^{TT} \\ (c_{e\tau}^{TT})^* & (c_{\mu\tau}^{TT})^* & 0 \end{pmatrix}$$

Eigenvalues:

$$E_i = -2\sqrt{Q}\cos\left(\frac{\theta_i}{3}\right) - \frac{a}{3}$$

$$\begin{aligned} Q =& \frac{a^2 - 3b}{9} \\ \theta_0 =& \cos^{-1}\left(RQ^{-\frac{3}{2}}\right) \\ \theta_1 =& \theta_0 + 2\pi \\ \theta_2 =& \theta_0 - 2\pi, \end{aligned}$$

$$\begin{aligned} a =& -\operatorname{Tr}(H) \\ b =& \frac{\operatorname{Tr}(H)^2 - \operatorname{Tr}(H^2)}{2} \\ c =& -\det(H) \\ R =& \frac{2a^3 - 9ab + 27c}{54}. \end{aligned}$$

Special Thanks:

J.S. Diaz of IU

Calculation of LV Oscillation Probabilities

Hamiltonian:

$$H = U \begin{pmatrix} 0 & 0 & 0 \\ 0 & \frac{\Delta m^2_{21}}{2E} & 0 \\ 0 & 0 & \frac{\Delta m^2_{31}}{2E} \end{pmatrix} U^\dagger \pm \sqrt{2} G_F \begin{pmatrix} N_e & 0 & 0 \\ 0 & 0 & 0 \\ 0 & 0 & 0 \end{pmatrix} \pm \begin{pmatrix} 0 & a^T_{e\mu} & a^T_{e\tau} \\ (a^T_{e\mu})^* & 0 & a^T_{\mu\tau} \\ (a^T_{e\tau})^* & (a^T_{\mu\tau})^* & 0 \end{pmatrix} - E \begin{pmatrix} 0 & c^{TT}_{e\mu} & c^{TT}_{e\tau} \\ (c^{TT}_{e\mu})^* & 0 & c^{TT}_{\mu\tau} \\ (c^{TT}_{e\tau})^* & (c^{TT}_{\mu\tau})^* & 0 \end{pmatrix}$$

Eigenvalues:

$$E_i = -2\sqrt{Q}\cos\left(\frac{\theta_i}{3}\right) - \frac{a}{3}$$

$$\begin{aligned} Q =& \frac{a^2 - 3b}{9} \\ \theta_0 =& \cos^{-1}\left(RQ^{-\frac{3}{2}}\right) \\ \theta_1 =& \theta_0 + 2\pi \\ \theta_2 =& \theta_0 - 2\pi, \end{aligned}$$

$$\begin{aligned} a =& -\operatorname{Tr}(H) \\ b =& \frac{\operatorname{Tr}(H)^2 - \operatorname{Tr}(H^2)}{2} \\ c =& -\det(H) \\ R =& \frac{2a^3 - 9ab + 27c}{54}. \end{aligned}$$

Special Thanks:

J.S. Diaz of IU

Calculation of LV Oscillation Probabilities

Hamiltonian:

$$H = U \begin{pmatrix} 0 & 0 & 0 \\ 0 & \frac{\Delta m^2_{21}}{2E} & 0 \\ 0 & 0 & \frac{\Delta m^2_{31}}{2E} \end{pmatrix} U^\dagger \pm \sqrt{2} G_F \begin{pmatrix} N_e & 0 & 0 \\ 0 & 0 & 0 \\ 0 & 0 & 0 \end{pmatrix} \pm \begin{pmatrix} 0 & a^T_{e\mu} & a^T_{e\tau} \\ (a^T_{e\mu})^* & 0 & a^T_{\mu\tau} \\ (a^T_{e\tau})^* & (a^T_{\mu\tau})^* & 0 \end{pmatrix} - E \begin{pmatrix} 0 & c^{TT}_{e\mu} & c^{TT}_{e\tau} \\ (c^{TT}_{e\mu})^* & 0 & c^{TT}_{\mu\tau} \\ (c^{TT}_{e\tau})^* & (c^{TT}_{\mu\tau})^* & 0 \end{pmatrix}$$

Eigenvalues:

$$E_i = -2\sqrt{Q} \cos\left(\frac{\theta_i}{3}\right) - \frac{a}{3}$$

$$\begin{aligned} Q &= \frac{a^2 - 3b}{9} \\ \theta_0 &= \cos^{-1}\left(R Q^{-\frac{3}{2}}\right) \\ \theta_1 &= \theta_0 + 2\pi \\ \theta_2 &= \theta_0 - 2\pi, \end{aligned}$$

$$\begin{aligned} a &= -\operatorname{Tr}(H) \\ b &= \frac{\operatorname{Tr}(H)^2 - \operatorname{Tr}(H^2)}{2} \\ c &= -\det(H) \\ R &= \frac{2a^3 - 9ab + 27c}{54}. \end{aligned}$$

Special Thanks:

J.S. Diaz of IU

LV Parameter		95% Upper Limit	Best Fit	No LV $\Delta\chi^2$	Previous Limit
$e\mu$	$\mathrm{Re}\left(a^T\right)$	1.8×10^{-23} GeV	1.0×10^{-23} GeV	1.4	4.2×10^{-20} GeV [51]
	$\mathrm{Im}\left(a^T\right)$	1.8×10^{-23} GeV	4.6×10^{-24} GeV		
	$\mathrm{Re}\left(c^{TT}\right)$	1.1×10^{-26}	1.0×10^{-28}	0.0	9.6×10^{-20} [51]
	$\mathrm{Im}\left(c^{TT}\right)$	1.1×10^{-26}	1.0×10^{-28}		
$e\tau$	$\mathrm{Re}\left(a^T\right)$	4.1×10^{-23} GeV	2.2×10^{-24} GeV	0.0	7.8×10^{-20} GeV [52]
	$\mathrm{Im}\left(a^T\right)$	2.8×10^{-23} GeV	1.0×10^{-28} GeV		
	$\mathrm{Re}\left(c^{TT}\right)$	1.2×10^{-24}	1.0×10^{-28}	0.3	1.3×10^{-17} [52]
	$\mathrm{Im}\left(c^{TT}\right)$	1.4×10^{-24}	4.6×10^{-25}		
$\mu\tau$	$\mathrm{Re}\left(a^T\right)$	6.5×10^{-24} GeV	3.2×10^{-24} GeV	0.9	–
	$\mathrm{Im}\left(a^T\right)$	5.1×10^{-24} GeV	1.0×10^{-28} GeV		
	$\mathrm{Re}\left(c^{TT}\right)$	5.8×10^{-27}	1.0×10^{-28}	0.1	–
	$\mathrm{Im}\left(c^{TT}\right)$	5.6×10^{-27}	1.0×10^{-27}		

TABLE II. Summary of the results of the six fits for Lorentz-violating parameters (the real and imaginary parts of each parameter are fit simultaneously. The 95% upper limits and best fits are shown, as well as the $\Delta\chi^2$ for no Lorentz violation. The most significant exclusion of No LV is $a^T_{e\mu}$, which still includes No LV within the 68% C.L. Since the parameters are scanned on a logarithmic scale, 10^{-28} is the minimum value considered and is equivalent to no LV.